

# Two trapped particles interacting by a finite-ranged two-body potential in two spatial dimensions

Md Hamid<sup>1,\*</sup> and M.A.H. Ahsan<sup>1</sup>

<sup>1</sup>*Department of Physics, Jamia Millia Islamia  
(Central University), New Delhi 110025, India.*

## Abstract

We examine the problem of two particles confined in an isotropic harmonic trap, which interact via a finite-ranged Gaussian-shaped potential in two spatial dimensions. We derive an approximate transcendental equation and solved it using exact diagonalization to study the resulting energy spectrum as a function of the inter-particle interaction strength, relative angular momenta and analyse the role of Hilbert space. Both the attractive and repulsive systems are analysed. We study the impact of the potential's range on the ground-state energy. Complementary, we also explicitly verify by a variational treatment that in the zero-range limit the positive delta potential in two dimensions only reproduces the non-interacting results, if the Hilbert space is not truncated. Finally, we established and discuss the connection between our finite-range treatment and regularized zero-range results from the literature.

---

\* hamidjmi2008@gmail.com

## I. INTRODUCTION

The theoretical prediction of Bose-Einstein condensation goes back to a century ago when Bose worked out the quantum statistics of photons[1] which lead Einstein to make theoretical background for the non-interacting massive bosons that at below a certain finite but small temperature a finite fraction of the total number of particles will occupy the single particle ground state[2]. Following this, F. London drew an analogy between the superfluidity of liquid  $^4\text{He}$  and Bose-Einstein condensation[3] that led to the further extension of the theoretical development.

The study of Exact solution of harmonically trapped two ultra cold spin-0 bosons in 2D interacting via finite range two body potential modelled by a Gaussian potential, has been shown to put vast interest in the last few decades in the field of optical lattices, quantum information and entanglement has been discuss for the two identical particles[4–6]. Many-body physics is rather complex when atom-atom interaction is considered. To avoid this complexity, one employs the contact potential. For spatial degree, the delta-function potential is suitable but for the higher dimension the choice of delta potential is not suitable fit because the Hamiltonian is not self-adjoint [7, 8]. The two-body system is rather easy and suitable test for study of the choice of single particle basis in terms of active Hilbert space and inter-particles interaction range  $\sigma$ , along with particle-particle interaction strength  $g_2$ . In the present article, we discussed the choice of finite range over contact potential in both interaction range. In BECs, quantum mechanics emerges at macroscopic scales. It has led to a better understanding of other phenomena of condensed matter physics like superfluidity, phase transition, symmetry breaking etc. The Bose-Einstein condensation of alkali vapours at nano-kelvin temperatures is the main interest of the present article.

In this chapter, we investigate the role of relative angular momentum  $m$ , single particle basis state or active Hilbert state ( $\tilde{N}_c$ ), inter-particle interaction strength  $g_2 > 0$  and  $< 0$ , interaction range  $\sigma$ , in the system of two spin-0 bosons i.e.  $N = 2$  interacting via a finite range two body potential modelled by a Gaussian potential. In the quasi two dimensional space, two spin-0 bosons interacting via a finite range Gaussian potential exposed to external trap potential which provides rotation to the system about a stiffer z-axis, within the system sizes. We construct the Hamiltonian and set up the analytical solution and diagonalise it using exact diagonalization. Few lower energy-states are being calculated to

study the role of interaction strength, range of systems etc. Obtaining the exact numerical results are challenging task, because of the rounding off errors. That's why we employ Exact Diagonalization. Variation of average energy spectrum with interaction range  $\sigma$  and zero relative angular momentum is studied, where the energy per particles first increases and the decreases within the system size[9], Variation of Hilbert space with decreasing interaction strength  $g_2 > 0$  for many-body systems in this article[10]. Dependence of single particle energy spectrum with angular momentum quantum number is discussed for spin-1 bosons where energy increases linearly for higher relative particle angular momentum  $m$ [11, 12], later discussed the different relative angular momentum in attractive BECs . The role of relative particle angular momentum has been discussed for fermionic systems is also studied for the few-particles [13].

We can tune the scattering length  $a_s$  for both attractive as well as repulsive strength, by Feshbach resonances[14–16] and hence the two particles interaction parameters  $g_2$  can also be tuned accordingly, for  $a_s < 0$  the  $g_2$  is attractive and repulsive for  $a_s > 0$ . For the limit  $\sigma \rightarrow 0$  the effective potential tends to a contact potential  $g_2\delta(\mathbf{r})$  which has been studied extensively for example [17].

We organize this paper as follows. In Sec. II, we derive the general secular Hamiltonian equation for the energy of two trapped spin-0 particles interacting via a normalized Gaussian-shaped two-body interacting potential in 3D which is being reduces it to quasi 2D counterpart. In Sec. III, we derive the relation for the contact potential and studied the leading spectrum and role of active Hilbert space. Sec. IV, we established the finite range potential, a general relation in IV A and an explicit relation in IV B of the article which deals with the numerical results related to the different ground states. In Sec. V, in this section we present our findings. Finally, in Sec. VI we offer a summary and conclusion of our findings. Supplemental derivations and numerics are deterred to the appendices.

## II. THE HAMILTONIAN

We consider a system of  $N = 2$  spin-0 bosons, each of mass  $M$  in an external harmonic trap, which are interacting via a normalized Gaussian potential in a  $x - y$  symmetric two-dimensional plane with an externally impressed rotation  $\mathbf{\Omega} = \Omega\hat{z}$  about  $z$ -axis, has been studied in the recent years [8, 18–21] are the bench mark for our study. The Hamiltonian

of this system in co-rotating frame can be written as,

$$\begin{aligned}
\widehat{\mathbf{H}}^{rot} &= \widehat{\mathbf{H}}^{lab} - \widehat{\mathbf{\Omega}} \cdot \widehat{\mathbf{L}}^{lab} \\
\widehat{\mathbf{H}}^{lab} &= \sum_{i=1}^N \left[ \frac{\widehat{\mathbf{p}}_i^2}{2M} + \frac{1}{2} M \omega_{\perp}^2 (r_{\perp i}^2 + \lambda_z^2 z_i^2) \right] + g_2 \left( \frac{1}{\sqrt{2\pi}\sigma} \right)^3 \\
&\quad \times \sum_{i \neq j} \exp\left(-\frac{1}{2\sigma^2} ((r_{\perp i} - r_{\perp j})^2 + (z_i - z_j)^2)\right)
\end{aligned} \tag{1}$$

here  $g_2 = \frac{4\pi a_s}{a_{\perp}}$ , is the interaction strength,  $\omega_{\perp}$  is harmonic oscillator strength,  $a_{\perp}$  is harmonic oscillator length,  $a_s$  is the s-wave scattering length and  $\sigma$  is the range of two body interaction parameter. The two-particles interaction strength  $g_2$  and interaction range parameter  $\sigma$  are in units of  $\hbar\omega$  and  $\sqrt{\hbar/M\omega}$  respectively,  $\mathbf{r}$  and  $\mathbf{p}$  are the co-ordinate and conjugate momenta respectively,  $r_{\perp} = (x, y)$  constitutes a plane,  $\widehat{\mathbf{L}}_z^{lab}$  is total angular momentum of the system and  $\mathbf{I}_z^{lab} = m$  is relative particle angular momentum unless it is specified and its eigenvalues will read in Lab frame only.

We have observed that for  $|m| = 0$ , as we go from repulsive to attractive interaction, the  $E_0$  decreases. Apart from this observation, one crucial observation is, there is  $E_0(N)$ , for  $g_2 = -1$  the size of single particle basis (as function of Hilbert space) increases toward infinite (in online colour light yellow) as contrast to the positive  $g_2 = +1, +2, +3$  and  $+4$ , where, the size of single particle basis becomes finite in size for a small number of Hilbert space, shown in Fig. 1, and for  $|m| = 1$ , the size of basis state is infinite for  $g_2 = -4$  in contrast to  $g_2 = -1$ . We observed that the choice of interaction strength,  $g_2 = +1, +2, -1$  and  $-2$  are the best choice for the study, Fig. 2. As we know that the Gaussian potential in Eq. 1, can be expanded within the finite number of single particle basis in contrast to the contact potential which takes infinite size in terms of single particle basis. For relative angular momentum  $|m| = 0$ , size of basis state tends toward infinite in the case of  $\sigma = 0.001, 0.1$ , and  $0.3$  but in the range  $\sigma = 0.4$  to  $0.9$ , the basis size becomes finite, which is evident from the Fig. 3. For single particles angular momentum  $|m| = 1$ , the size of basis state is finite over all range of  $\sigma$ , which is evident from the Fig. 4 and in Table as well I hence we conclude that the choice of finite range potential is a good choice over the contact potential. Selection of active Hilbert space(single particle basis) is chosen for the construction for the two-particles system[32].

Variational method is used to calculate the eigenenergy. We have chosen variational

symmetric basis function (bosons) for our system which has  $x - y$  rotational symmetry assuming  $\lambda_z \equiv \frac{\Omega_z}{\Omega_\perp}$  a highly oblate spheroidal that turns the angular momentum  $L_z$ , is a good quantum number. The system is considered as an effective 2-D harmonic oscillator with energy  $\hbar\omega_\perp$ , where,  $\omega_\perp$  is radial confining frequency defined in terms of the inverse squared harmonic oscillator length  $\alpha$ , is  $\omega_\perp = \frac{\hbar}{M\alpha^{-2}}$  and the harmonic oscillator length is defined as  $a_\perp = 1/\alpha$ .

The Hamiltonian can be separated in  $x - y$  plane as  $\hat{h}_\perp$  and  $z$ -component as  $\hat{h}_z$  as there is no excitation along the stiffer  $z$ -axis and hence behaves as frozen.

$$\begin{aligned}\hat{\mathbf{h}} &= \underbrace{\frac{\hat{\mathbf{p}}_\perp^2}{2M} + \frac{M\omega_\perp^2 r_\perp^2}{2}}_{\hat{h}_\perp} - \hat{\mathbf{L}} \cdot \hat{\boldsymbol{\Omega}} + \underbrace{\frac{\hat{p}_z^2}{2M} + \frac{M\omega_z^2 z^2}{2}}_{\hat{h}_z} \\ &\equiv \hat{h}_\perp + \hat{h}_z\end{aligned}$$

the eigen-solution for  $\hat{h}_z$  is

$$\hat{h}_z \Psi = \epsilon_{n_z} \Psi$$

with,  $\epsilon_{n_z} = (n_z + \frac{1}{2}) \hbar\omega_z$ ,  $n_z = 0$

### A. THE EIGEN-SOLUTION IN QAUSI 2D SYSTEMS

Writing the 2-D interaction Hamiltonian for two spin-0 bosons in relative co-ordinates system in terms of reduced mass  $\mu$  and total mass  $M$  will be of the following form.

$$\begin{aligned}\hat{\mathbf{H}}_{\text{rel}} &= \sum_1^2 \left( \frac{-\hbar}{2\mu} \nabla_i^2 + \frac{1}{2} \mu \omega^2 \hat{\mathbf{r}}^2 \right) + g_2 V(\hat{\mathbf{r}}) - \hat{\boldsymbol{\Omega}} \cdot \hat{\mathbf{L}} \\ \hat{\boldsymbol{\Omega}} \cdot \hat{\mathbf{L}} &= \hat{\boldsymbol{\Omega}} (\hat{\mathbf{R}} \times \hat{\mathbf{P}} + \hat{\mathbf{r}} \times \hat{\mathbf{p}}) \\ V(\hat{\mathbf{r}}) &= \left( \frac{1}{\sqrt{2\pi}\sigma} \right)^2 \sum_{i \neq j} \exp \left( -\frac{1}{2\sigma^2} (r_{\perp i} - r_{\perp j})^2 \right)\end{aligned}\tag{2}$$

Here,  $\nabla$  is the 2-D Nabla operator, the problem is reduced in center of mass  $\mathbf{R} = \frac{1}{2}(\mathbf{r}_1 + \mathbf{r}_2)$  and relative co-ordinate system  $\mathbf{r} = \mathbf{r}_1 - \mathbf{r}_2$

$$\begin{aligned}\hat{\mathbf{H}} &= \hat{\mathbf{H}}_{\text{com}} + \hat{\mathbf{H}}_{\text{rel}} \\ \hat{\mathbf{H}}_{\text{com}} &= -\frac{\hbar^2}{2M} \nabla_R^2 + \frac{1}{2} M \omega^2 \mathbf{R}^2\end{aligned}$$

$$\hat{\mathbf{H}}_{\text{rel}} = \underbrace{-\frac{\hbar^2}{2\mu}\nabla_r^2 + \frac{1}{2}\mu\omega_{\perp}^2\hat{\mathbf{r}}^2 - \hat{\mathbf{\Omega}} \cdot \hat{\mathbf{L}}}_{H_{\text{SP}}} + g_2 V(\hat{\mathbf{r}}) \quad (3)$$

non-interacting COM motion is explicitly removed. [23]

## B. SOLUTION FOR THE INTERACTION HAMILTONIAN

We start constructing the solution for the Hamiltonian in relative co-ordinates system. A secular equation is established to study the quantities of interest in the following manner,

$$\hat{\mathbf{H}}_{\text{rel}} \Psi = \hat{\mathbf{E}} \Psi$$

where,

$$\Psi = \sum_{n_r, m}^{\infty} c_{n_r, m} u_{n_r, m} \quad (4)$$

Solution for relative Hamiltonian<sup>3</sup> consists of single particle Hamiltonian  $H_{\text{SP}}$  and the interaction Hamiltonian consists of normalized Gaussian interaction potential. Starting from finite size of single particle basis state. The eigenstate  $\Psi$  can be expanded in linear sum of single particle basis states as,  $\Psi = \sum_{n_r, m}^{\infty} c_{n_r, m} |u_{n_r, m}\rangle$  with relative particle angular momentum  $m$  and rotational quantum number  $n_r$ , on the Schödinger equation. For the Hamiltonian  $H_{\text{SP}}$  of the system, the eigen-energy are of the form of  $\epsilon_{n_r, m} = 2n_r + 1 + |m|$  and eigen-spectrum for the relative Hamiltonian<sup>3</sup> is given below in Eq.(5) is known as the secular equation. Secular equation is being set up in the following manner, on  $H_{\text{rel}}|\Psi\rangle = E|\Psi\rangle$ , projecting  $|u_{n_r', m}\rangle$  from left, sets up secular equation:

$$c_{n_r', m}(\epsilon_{n_r', m} - E) + g_2 \sum_{n_r, n_r'=0}^{\infty} c_{n_r, m} \int_0^{\infty} \int_0^{2\pi} \times u_{n_r', m}^*(r, \phi) V(r) u_{n_r, m}(r, \phi) r dr d\phi = 0$$

writing the above equation in the compact form,

$$c_{n_r', m}(\epsilon_{n_r', m} - E) + g_2 \sum_{n_r, n_r'=0}^{\infty} c_{n_r, m} I_{n_r, n_r', |m|}(\sigma) = 0 \quad (5)$$

where,  $I_{n_r, n_r', |m|}(\sigma) = \int_0^{\infty} \int_0^{2\pi} u_{n_r', m}^*(r, \phi) V(r) u_{n_r, m}(r, \phi) r dr d\phi$

in which the interaction matrix elements,  $I_{n_r, n_{r'}, |m|}(\sigma)$  is solved in appendix A and  $c_{n_r, m}$  is given in appendix B. The matrix elements in Eq.(5) is in the terms of interaction range  $\sigma$  and inverse harmonic oscillator length  $\alpha$  is evaluated by means of Exact Diagonalization[24].

$$\begin{aligned}
I_{n_r, n_{r'}, |m|}(\sigma) &= \frac{(\alpha^2)^{1+|m|} (2\sigma^2)^{|m|}}{\pi(1 + 2\alpha^2\sigma^2)^{n_r+n_{r'}+|m|+1}} \\
&\times \sqrt{\frac{n_r!}{(n_r + |m|)!} \frac{n_{r'}!}{(n_{r'} + |m|)!}} \\
&\times \sum_{i=0}^{\min(n_r, n_{r'})} \binom{|m| + n_r}{|m| + i} \binom{|m| + n_{r'}}{|m| + i} \\
&\times \frac{(|m| + i)!}{i!} (2\alpha^2\sigma^2)^{2i}.
\end{aligned} \tag{6}$$

for zero-relative angular  $|m| = 0$ , the above Eq.(6) simplifies to the following relation which matches with [8],

$$\begin{aligned}
I_{n_r', n_r, 0}(\sigma) &= \frac{\alpha^2}{\pi} \left( \frac{1}{1 + 2\alpha^2\sigma^2} \right)^{n_r+n_r'+1} \\
&\times {}_2F_1(-n_r', -n_r; 1, 4(\alpha\sigma)^4)
\end{aligned} \tag{7}$$

where,

$$\alpha = \sqrt{\frac{\mu\omega_{\perp}}{\hbar}} \text{ and } {}_2F_1 \text{ is Gauss-Hypergeometric function.}$$

### III. SOLUTION FOR THE CONTACT POTENTIAL

Before we start the finite range study, we first explore the case  $\sigma \rightarrow 0$  in which the normalized Gaussian potential defined in Eq.(1) behaves like a contact potential. Following the Eq. (1), for the rotating case, the relative angular momentum ( $m \neq 0$ ), the interaction matrix elements becomes  $I_{n_r', n_r, m}(0) = 0$ , means do not feel the zero range interaction and for non-rotating case ( $m = 0$ ) the interaction matrix elements  $I_{n_r', n_r, 0}(0) = \alpha^2/\pi$ , a constant, thus the Eq. (5) becomes,

$$c_{n_r', 0}(\epsilon_{n_r', 0} - E) + g_2 \sum_{n_r=0}^{\infty} c_{n_r, 0} \frac{\alpha^2}{\pi} = 0 \tag{8}$$

using the variational calculation, we can find the form of  $c_{n_r',0} = -\frac{g_2 C}{\epsilon_{n_r',0} - E}$ , here  $C$  is again a constant, rearranging the above Eq. (8), we get the energy relation. Truncating the summation to a finite size of Hilbert space  $\tilde{N}$ , and studying the energy spectrum for the critical Hilbert space  $\tilde{N}_c$ .

$$\frac{\pi}{\alpha^2} + g_2 \sum_{n_r=0}^{\tilde{N}_c} \frac{1}{\epsilon_{n_r,0} - E} = 0$$

writing  $\epsilon_{n_r,0} = (2n_r + 1)\hbar\omega$  and making the above equation dimensionless,

$$\frac{\pi}{\alpha^2} + \frac{g_2}{\hbar\omega_\perp} \sum_{n_r=0}^{\tilde{N}_c} \frac{1}{2n_r + 1 - E/\hbar\omega_\perp} = 0 \quad (9)$$

from above equation, setting  $\alpha = 1$ , we can get the information about the energy spectrum of non-rotating two bosons interacting via contact potential as function of Hilbert space, which further will give the idea of active Hilbert space. Figs. 1,2,3, 4,5 and 6 has been discussed below.

#### IV. FINITE-RANGE POTENTIAL

##### A. SOLUTION FOR FINITE RANGE POTENTIAL, MOST GENERAL FORM

Solution for relative Hamiltonian consists of single particle Hamiltonian  $H_{\text{SP}}$  and the interaction Hamiltonian consists of normalized Gaussian interaction potential. Using the eigenstate  $\Psi$  in terms of linear sum of single particle basis states  $\Psi = \sum_{n_r,m} c_{n_r,m} |u_{n_r,m}\rangle$  with relative particle angular momentum  $m$ , on the Schödinger equation.

$$c_{n_r,m} = -\frac{g_2 \langle u_{n_r,m} | W | \Psi \rangle}{(\epsilon_{n_r,m} - E)} \quad (10)$$

We choose  $|\Psi\rangle = |\phi_{n_r'}\rangle$  to study the higher excited states and  $|\Psi\rangle = |\phi_0\rangle$  for the ground state energy. Substituting the above Eq. (10) in Eq. (5) for the former case after rearranging the terms gives the following relation,

$$I_{n_r,n_r',m}(\sigma) + \frac{g_2}{\hbar\omega_\perp} \times \sum_{n_r,n_r'}^{\min(n_r,n_r')} \frac{I_{n_r,n_r',|m|}^2(\sigma)}{2n_r + |m| + 1 - m\Omega/\omega_\perp - E/\hbar\omega_\perp} = 0$$

the above equation is solved numerically for the energy spectrum  $E$  in unit of  $\hbar\omega_\perp$ . Some of the results are shown in the following figures.



## B. SOLUTION FOR FINITE RANGE POTENTIAL

In order to study the finite range effects on a two particles system interacting via a normalized Gaussian potential, we first calculate the constant parameter using perturbation theory in Appendix B, a similar expression as calculated in previous section but not the same,

$$c_{n_r,m} = -\frac{g_2 \langle u_{n_r,m} | W | u_{n_{r'},m} \rangle}{(\epsilon_{n_r,m} - E)} \quad (11)$$

substituting  $n_{r'} = 0$  in Eq. (6) to get  $I_{0,n_r,m}$  and hence the above expression becomes,

$$c_{n_r,m} = \frac{-g_2}{\epsilon_{n_r,m} - E} I_{0,n_r,m}(\sigma) C \quad (12)$$

substituting the above expression in Eq. (5), sets-up an equation,

$$\begin{aligned} & \frac{-g_2}{(\epsilon_{n_{r'},m} - E)} (\epsilon_{n_{r'},m} - E) I_{0,n_{r'},m}(\sigma) C + \\ & g_2 \sum_{n_r}^{\infty} \frac{-g_2}{\epsilon_{n_r,m} - E} I_{0,n_r,m}(\sigma) C I_{n_r,n_{r'},m}(\sigma) = 0 \end{aligned}$$

simplify to,

$$\begin{aligned} I_{0,n_{r'},m}(\sigma) + g_2 \sum_{n_r}^{\infty} \frac{1}{\epsilon_{n_r,m} - E} I_{0,n_r,m}(\sigma) \\ \times I_{n_r,n_{r'},m}(\sigma) = 0 \end{aligned} \quad (13)$$

substituting  $n_{r'} = 0$

$$I_{0,0,m}(\sigma) + g_2 \sum_{n_r}^{\infty} \frac{1}{\epsilon_{n_r,m} - E} I_{0,n_r,m}^2(\sigma) = 0 \quad (14)$$

substituting the following two Eqs. (15) and (16) obtained from the Eq. (6) into above Eq. (14), simplify to the below final expression, Eq. (17) of this article.

$$I_{0,0,m}(\sigma) = \frac{(\alpha^2)^{1+|m|} (2\sigma^2)^{|m|}}{\pi (1 + 2\alpha^2\sigma^2)^{1+|m|}} \quad (15)$$

and

$$\begin{aligned} I_{0,n_r,m}(\sigma) &= \sqrt{\frac{n_r!}{(n_r + |m|)! (|m|)!}} \\ &\times \frac{(\alpha^2)^{1+|m|} (2\sigma^2)^{|m|}}{\pi (1 + 2\alpha^2\sigma^2)^{1+n_r+|m|}} \frac{(|m| + n_r)!}{n_r!} \end{aligned}$$

(16)

thus final expression becomes,

$$\begin{aligned}
& \frac{\pi (|m|!)^2}{(2\sigma^2)^{|m|}(\alpha^2)^{1+|m|}} (1 + 2\alpha^2\sigma^2)^{1+|m|} + \frac{g_2}{\hbar\omega_\perp} \\
& \times \sum_{n_r=0}^{\infty} \frac{1}{2n_r + 1 + |m| - E/\hbar\omega_\perp - m\hbar\Omega/\omega_\perp} \\
& \times \left( \frac{1}{1 + 2\alpha^2\sigma^2} \right)^{2n_r} \frac{(|m| + n_r)!}{n_r!} = 0
\end{aligned}
\tag{17}$$

the above equation is the main analytical result of the article. We can study the system for general relative angular momentum  $|m| = 0, \pm 1, \pm 2 \dots$ . For study purpose, we choose here only two values i.e. 0 and 1. For 0, the above equation is express in terms of Lerch transcendent function  $\Phi$ , as follow

$$\frac{\hbar\omega_\perp}{g_2} = -\frac{\alpha^2}{2\pi(1 + 2\alpha^2\sigma^2)} \Phi \left[ \frac{1}{(1 + 2\sigma^2\alpha^2)^2}, 1, \frac{1 - E/\hbar\omega_\perp}{2} \right]
\tag{18}$$

## V. NUMERICAL RESULTS AND DISCUSSION

For  $^{87}\text{Rb}$  atom, the size of the system turns out to be  $a_\perp = \sqrt{\frac{\hbar}{M\omega_\perp}} = 733$  nm with  $\omega_\perp = 2\pi \times 220$  Hz. The dimensionless interaction parameter  $g_2 = \frac{4\pi a_s}{a_\perp}$ , where  $a_s$  is the s-wave scattering length, is taken in the range  $-4$  to  $+4$  in the present study, the parameter  $g_2$  is a measure of the strength of the interaction. The energy spectrum for different values of the interaction range  $\sigma$  and the interaction strength  $g_2$  (attractive and repulsive) is being examined to study the active Hilbert space or number of basis states required for variational calculation. Once the basis state is set up, the Hamiltonian is diagonalized to study the energy spectrum. Various components of the energy namely the interaction energy  $\langle V \rangle$ , the kinetic energy  $\langle KE \rangle$  and the potential energy  $\langle PE \rangle$  are also computed such that  $E = \langle V \rangle + \langle KE \rangle + \langle PE \rangle$ .

In Fig. 1, we present the ground state energy  $E_0$  vs size of the Hilbert space  $\tilde{N}$  for the pair in the relative co-ordinates. For zero relative angular momentum  $|m| = 0$ , the plot  $E_0$

		$g_2 = -1$		$g_2 = +1$	
$\sigma$	$E_{sat}$	Hilbert Space	$\tilde{N}_c$	$E_{sat}$	Hilbert Space $\tilde{N}_c$
0.1	0.4238	139		1.2044	107
0.2	0.6008	37		1.2261	25
0.4	0.7333	13		1.2172	12
0.6	0.8079	6		1.1779	4
0.8	0.8583	3		1.1374	4
0.9	0.8773	3		1.1203	2

TABLE I: Active(critical) Hilbert space  $\tilde{N}_c$  for different interaction range  $\sigma$  for relative angular momentum  $|m| = 0$  with interaction strength  $g_2$ . Shows the variation of critical Hilbert space  $\tilde{N}_c$  with increase in  $\sigma$ .

*vs*  $\tilde{N}$  are being shown. For the positive (repulsive) interaction strength  $g_2 = +1, +2, +3$  and  $+4$ , we observe an upward shift in the ground state energy with increase in interaction strength. Higher the interaction strength, higher the ground state energy. For a given value of  $g_2$ , there is a critical size of the Hilbert space  $\tilde{N}_c(g_2)$  beyond which the ground state energy saturates and becomes independent of size of the Hilbert space. The critical size of Hilbert space is a point beyond which the ground state energy  $E_0$  gets saturated for a given set of parameters. For example, for  $g_2 = +1$ , the saturated ground state energy is 1.206 at the critical size of Hilbert space  $\tilde{N}_c = 33$  and for  $g_2 = +4$ , the saturated ground state energy ( $E_{sat}$ ) is 1.396 at the critical size of Hilbert space  $\tilde{N}_c = 52$ . For the negative (attractive) interaction strength  $g_2 = -1$ , we observe that the ground state energy decreases with the increase with the size of Hilbert space and gets saturated at  $\tilde{N}_c = 81$  with  $E_{sat} = 0.425$ . Below  $g_2 < -1$ , the system becomes a lump and hence not being subjected to any statistical laws and consequently there is no need to study below  $-1$ . We also observed that the  $E_0$  is minimum for attractive interaction, most stable configuration. Writing the ground state energy  $E_0$  as function of  $E_0(E_{sat}, g_2, \tilde{N}_c)$ , as  $E_0(1.19, +1, 32)$  and  $E_0(1.396, +4, 52)$  in terms of increasing interaction. In Fig. 2, we present the study of ground state energy  $E_0$  *vs* size of the Hilbert space  $\tilde{N}$  for relative angular momentum  $|m| = 1$ . For the positive interaction strength  $g_2 = +1, +2, +3$  and  $+4$ , the ground state energy  $E_0$ , increases with increase in

$g_2$	$ m  = 0$		$ m  = 1$	
	$E_{sat}$	Hilbert space $\widetilde{N}_c$	$E_{sat}$	Hilbert space $\widetilde{N}_c$
-4	x	x	1.961	136
-3	x	x	1.975	72
-2	x	x	1.985	32
-1	0.425	81	1.993	04
1	1.206	33	2.006	06
2	1.309	25	2.010	26
3	1.361	39	2.015	28
4	1.396	52	2.018	47

TABLE II: Active Hilbert space  $\widetilde{N}_c$  for different interaction range  $\sigma$ , relative angular momentum  $|m| = 0$  and 1 and interaction strength  $g_2$ . For  $|m| = 0$  the zero-point energy is  $\hbar\omega$  and hence for  $g_2 < -1$  becomes un-physical system.

the interaction strength. The  $E_0$  gets saturated at a finite size of the Hilbert space. We can write the ground state energy  $E_0$ , as function of  $E_0(E_{sat}, g_2, \widetilde{N}_c)$ . We observed that, for higher  $g_2 = +4$ ,  $E_0(2.018, +4, 47)$  required more Hilbert space (single particle basis state) then for the lower  $g_2 = +1$ ,  $E_0(2.005, +1, 6)$  to become saturated.

For negative interaction strength  $g_2 = -1, -2, -3$  and  $-4$ , the ground state energy has negative shift with the decrease in interaction strength  $g_2$ . The critical size of Hilbert space  $\widetilde{N}_c$  increases with decrease in the interaction strength  $g_2$ , for example  $E_0(1.993, -1, 4)$ ,  $E_0(1.975, -3, 72)$  and  $E_0(1.961, -4, 136)$

We conclude that, for a given parameter ( $\sigma$ ), we have a range in which  $g_2$  can be varied to study the systems. In comparison to the Fig. 1, we observed that the saturation in the ground state energy has an upward shift with the change in the relative angular momentum  $|m|$ , from 0 to 1, for fixed interaction range  $\sigma$ , which is expected.

In Fig. 3, we present the study of ground state energy  $E_0$  vs size of the Hilbert space  $\widetilde{N}$  for relative angular momentum  $|m| = 0$ , the interaction strength  $g_2 = +1$  for the different values of interaction range  $\sigma$ . Here, we observed that the ground state energy has negative shift with the increase in interaction range  $\sigma$ . Further, we observed that for interaction

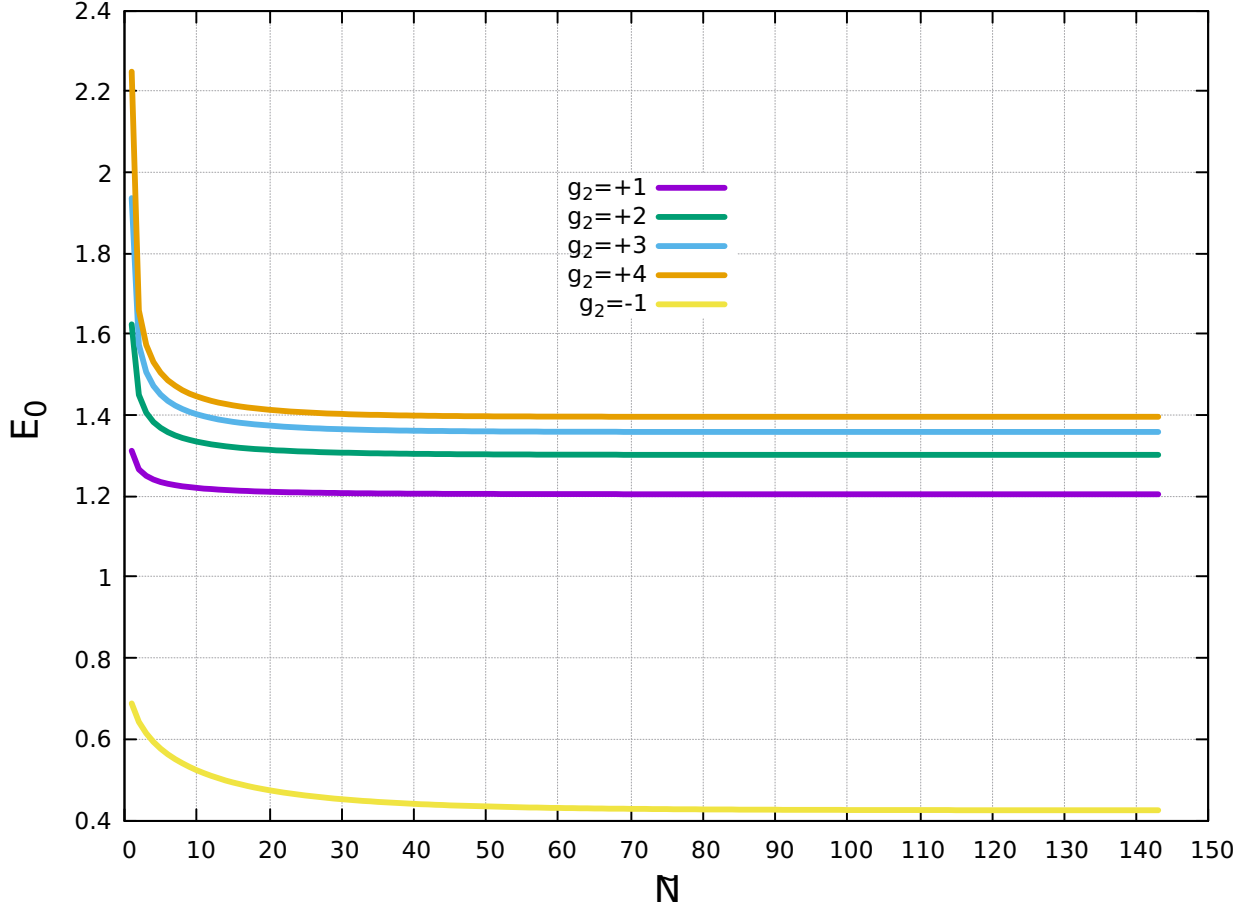


FIG. 1: (Colour online) Ground state energy ( $E_0$ ) in relative co-ordinates *vs* size of the Hilbert space ( $\tilde{N}$ ) for different values of interaction strength  $g_2$  and fixed value of interaction range  $\sigma = 0.1$  with zero-relative angular momentum  $|m| = 0$ . The quantities  $E_0$  and  $g_2$  are being measured in units of  $\hbar\omega$  and  $\hbar^2/m$  respectively.

range  $\sigma = 0.001$ , the nature of ground state energy  $E_0$  is asymptotic. In compact form  $E_0(E_{sat}, \sigma, \tilde{N}_c)$ , our observations conclude that as the interaction range  $\sigma$  increases, size of the critical Hilbert space decreases, here are some results in terms of increasing interaction range,  $E_0(1.226, 0.2, 14)$ ,  $E_0(1.228, 0.3, 7)$  and  $E_0(1.199, 0.5, 6)$ , which shows decreasing size of the critical Hilbert space respectively. It has been observed that the ground state energy gets well saturated in the case of higher interaction range i.e.  $\sigma = 0.3$  to  $0.9$  in contrast to the lower interaction range, say  $\sigma = 0.001$  to  $0.2$ . We observe that the use of finite range potential is the best suit for the computation over contact potential.

In Fig. 4, we present the study of ground state energy  $E_0$  *vs* size of the Hilbert space

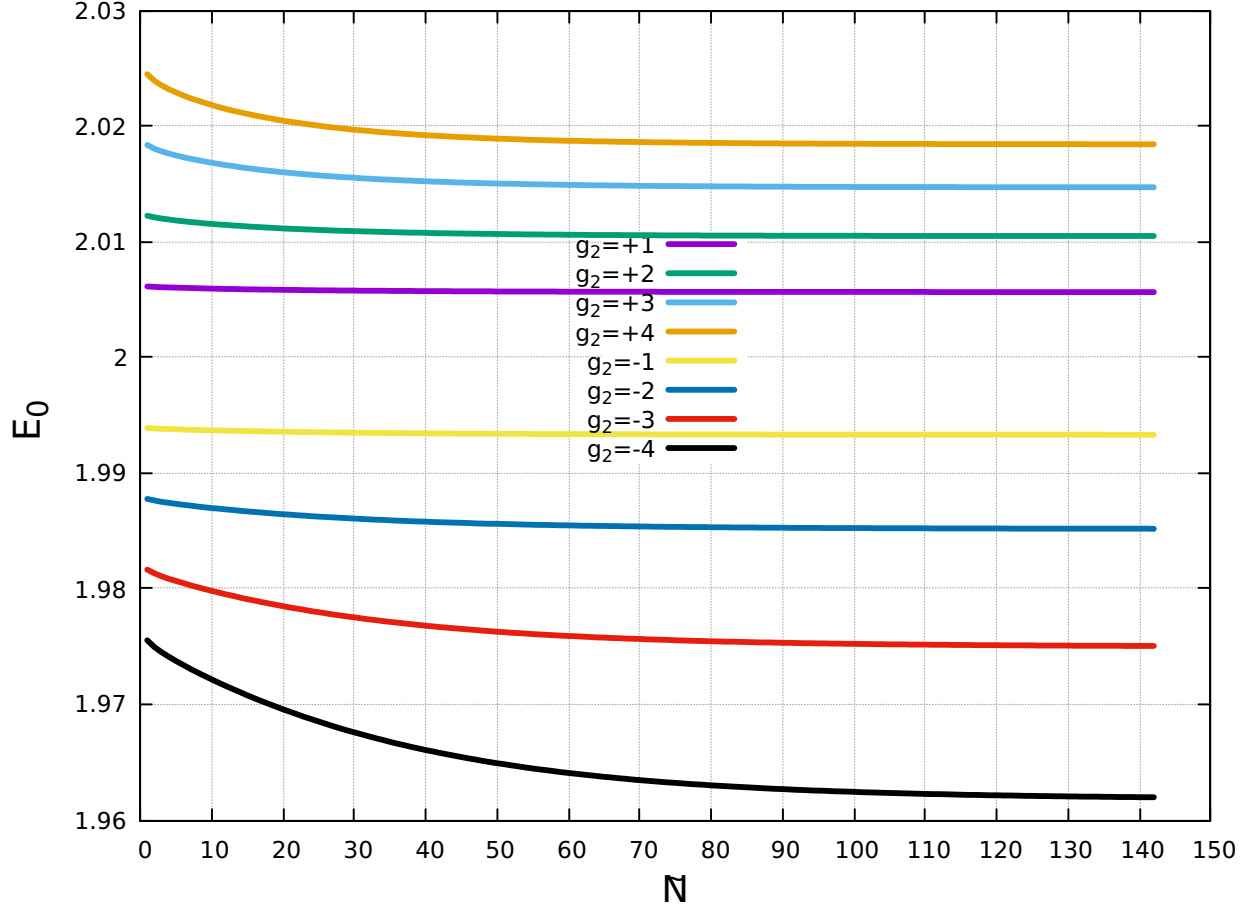


FIG. 2: (Colour online) Ground state energy  $E_0$  in relative co-ordinates *vs* size of the Hilbert space ( $\tilde{N}$ ) for different values of interaction strength  $g_2$  and fixed value of interaction range  $\sigma = 0.1$  with relative angular momentum  $|m| = 1$ . The quantities  $E_0$  and  $g_2$  are being measured in units of  $\hbar\omega$  and  $\hbar^2/m$  respectively.

$\tilde{N}$ , for a fixed value of interaction strength  $g_2 = +1$ , relative angular momentum  $|m| = 1$  and different values of interaction range  $\sigma$ . We observed that the ground state energy has increased with increase in the interaction range. When the ground state energy  $E_0$  is written as function of  $E_0(E_{sat}, \sigma, \tilde{N}_c)$ , with increasing interaction range  $\sigma$ ,  $E_0(2.0201, 0.2, 17)$  and  $E_0(2.6739, 0.5, 8)$ , size of critical Hilbert space decreases. We observed that for the interaction range  $\sigma = 0.0001$  and  $0.1$ , the ground state energy is saturated. We also observed that for the interaction range  $\sigma = 0.2$  and beyond energy first decreases and then becomes constant. The Hilbert space saturation point is reached at relatively smaller system size,  $\tilde{N} = 20$ . The study shows that ground state energy becomes independent of size of the

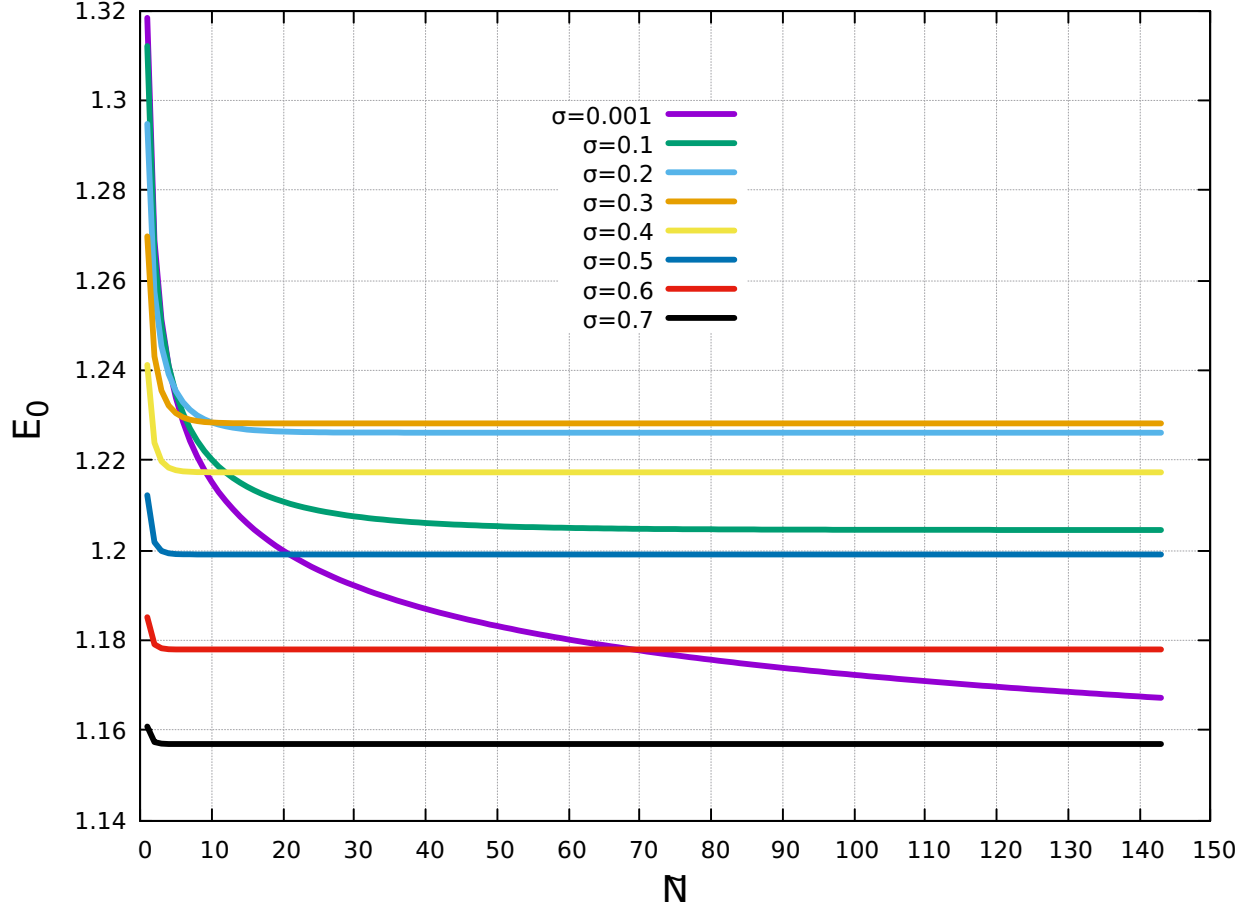


FIG. 3: (Colour online) Ground state energy  $E_0$  in the relative co-ordinate  $vs$  size of the Hilbert space  $\tilde{N}$  for different values of interaction range  $\sigma$  and a fixed value of interaction strength  $g_2 = +1$ , for relative angular momentum  $|m| = 0$ . The quantities  $E_0$  and  $\sigma$  are being measured in units of  $\hbar\omega$  and  $\sqrt{\frac{\hbar}{m\omega}}$  respectively.

Hilbert space around  $\tilde{N} = 20$  and hence the system does not require much basis state and computation becomes easier. In Fig. 5, we present the study of ground state energy  $E_0$   $vs$  size of the Hilbert space  $\tilde{N}$ , for negative interaction strength  $g_2 = -1$  and relative angular momentum  $|m| = 0$ . We observed that the  $E_0$  increases with increase in the  $\sigma$ . The nature of slope for  $E_0$  is divergent for  $\sigma = 0.001$ , the saturation for  $\sigma = 0.001$  is asymptotic in nature. Writing  $E_0$  in as function of  $E_0(E_{sat}, \sigma, \tilde{N}_c)$ , for increasing interaction range  $\sigma$ ,  $E_0(0.42, 0.1, 73)$  and  $E_0(0.77, 0.5, 6)$ , we conclude that the size of critical Hilbert space  $\tilde{N}_c$  decreases. In the case of  $\sigma = 0.4, 0.5, 0.7$  and  $= 0.9$ , the deviation in  $E_0$  is constant.

In this Fig. 6, we present the study of ground energy  $E_0$   $vs$  size of the Hilbert space  $\tilde{N}$ ,

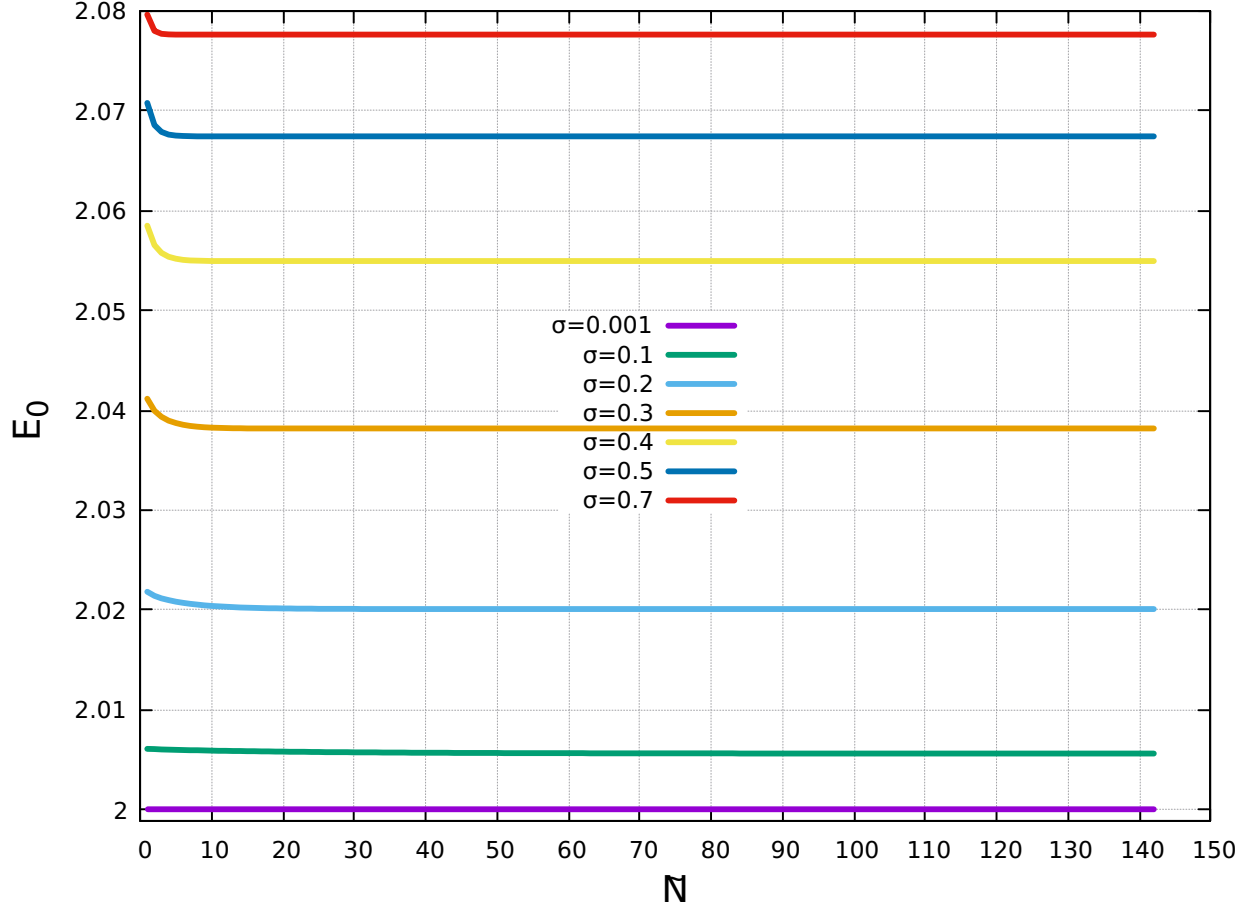


FIG. 4: (Colour online) Ground state energy  $E_0$  in the relative co-ordinate  $vs$  size of the Hilbert space  $\tilde{N}$  for different values of interaction range  $\sigma$  and a fixed value of interaction strength  $g_2 = +1$ , for relative angular momentum  $|m| = 1$ . The quantities  $E_0$  and  $\sigma$  are being measured in units of  $\hbar\omega$  and  $\sqrt{\frac{\hbar}{m\omega}}$  respectively.

for a fixed interaction strength parameter  $g_2 = -1$ , relative angular momentum  $|m| = 1$  and different interaction range  $\sigma$ . We have observed decrease in the ground state energy with increase in the interaction range  $\sigma$ .  $E_0$  in terms of increasing interaction range  $\sigma$ ,  $E_0(1.976, 0.2, 6)$   $E_0(1.956, 0.3, 3)$  indicates the decreasing size of critical Hilbert space,  $\tilde{N}_c$ .

In the Table I, we summarise the value of saturated ground state energy  $E_{sat}$ , against the interaction range  $\sigma$  for which the critical Hilbert space  $\tilde{N}_c$  is listed. We have observed that as interaction range increases the size of Hilbert space decreases for the given parameters.

In the Fig. 7, we present the study of energy spectrum  $E$ , in relative co-ordinates  $vs$  the interaction strength  $g_2$  for the relative angular momentum  $|m| = 0$  and 1. The first three



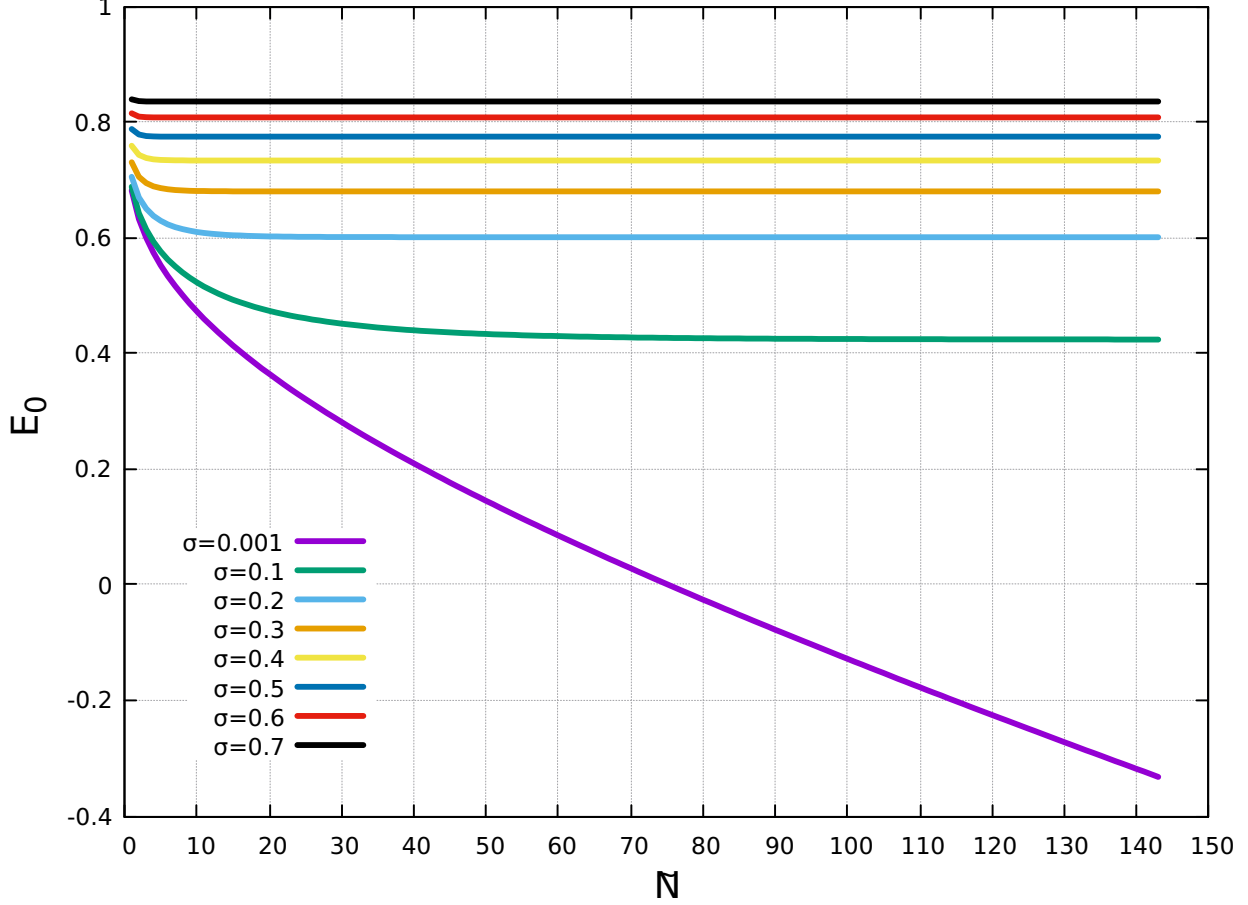


FIG. 5: (Colour online) The ground state energy  $E_0$  in relative co-ordinates *vs* size of Hilbert space  $\tilde{N}$  for the different values of interaction range  $\sigma$ , fixed attractive interaction strength  $g_2 = -1$  and relative angular momentum ( $|m| = 0$ ). The quantities  $E_0$  and  $\sigma$  are being measured in units of  $\hbar\omega$  and  $\sqrt{\frac{\hbar}{m\omega}}$  respectively.

energy in relative angular momentum  $m = 0$  ( $m = 1$ ), such as  $(E_0, m = 0)$ ,  $(E_1, m = 0)$  and  $(E_2, m = 0)$  ( $(E_0, m = 1)$ ,  $(E_1, m = 1)$  and  $(E_2, m = 1)$ ) correspond to ground state energy, first excited state energy and the second excited state energy respectively. The energy spectrum in the case of relative angular momentum  $|m| = 1$  has shown the non-dependence on the interaction strength parameter  $g_2$ . The ground state energy  $E_0$ , for relative angular momentum  $|m| = 0$ , in the attractive interaction range  $g_2 < 0$ , becomes negative and even diverged to  $-\infty$ , leaving the system un-physical, that is why we argued that the system is no more physical beyond the interaction strength  $g < -1$  and for  $g_2 > 0$  becomes degenerate over the range. At zero interaction strength, the energy difference between the consecutive

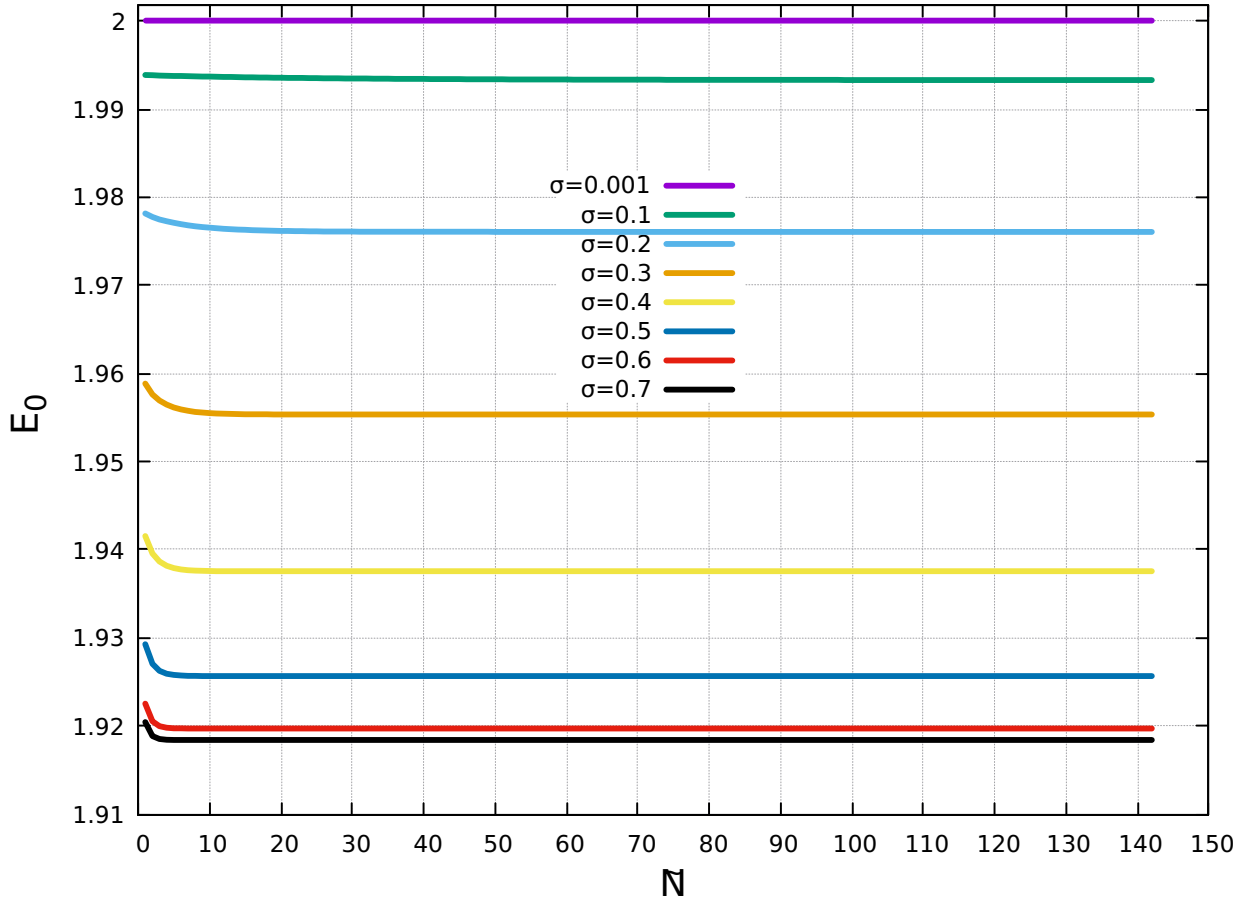


FIG. 6: (Colour online) Ground state energy  $E_0$  in the relative co-ordinate  $vs$  size of the Hilbert space  $\tilde{N}$  for different values of interaction range  $\sigma$  and a fixed value of interaction strength  $g_2 = -1$ , for relative angular momentum  $|m| = 1$ . The quantities  $E_0$  and  $\sigma$  are being measured in units of  $\hbar\omega$  and  $\sqrt{\frac{\hbar}{m\omega}}$  respectively.

energy levels i.e.  $E_1 - E_0 = E_2 - E_1 = 2\hbar\omega_{\perp}$  for both zero and non-zero relative angular momentum  $|m|$ , further, we recover the non-interacting energy  $E(n_r, |m|) = (2n_r + |m| + 1)\hbar\omega$ .

In Fig. 8, we plot the average interaction potential  $\langle V \rangle$   $vs$  interaction strength  $g_2$ , for relative angular momentum  $|m| = 0$  and interaction range  $\sigma = 0.1$ . We observed the similar trends to the 7 but not the same in the sense of energy gap. The  $\langle V_0 \rangle$ ,  $\langle V_1 \rangle$  and  $\langle V_2 \rangle$  are the ground, first and the second excited state energy respectively, in the range,  $g_2 < 0$  the ground state interaction energy,  $\langle V_0 \rangle$  is diverged to the infinity similar to  $E_0$ , rest of two energy has overlap in entire region. For  $g_2 > 0$  the all three energy has constant value.

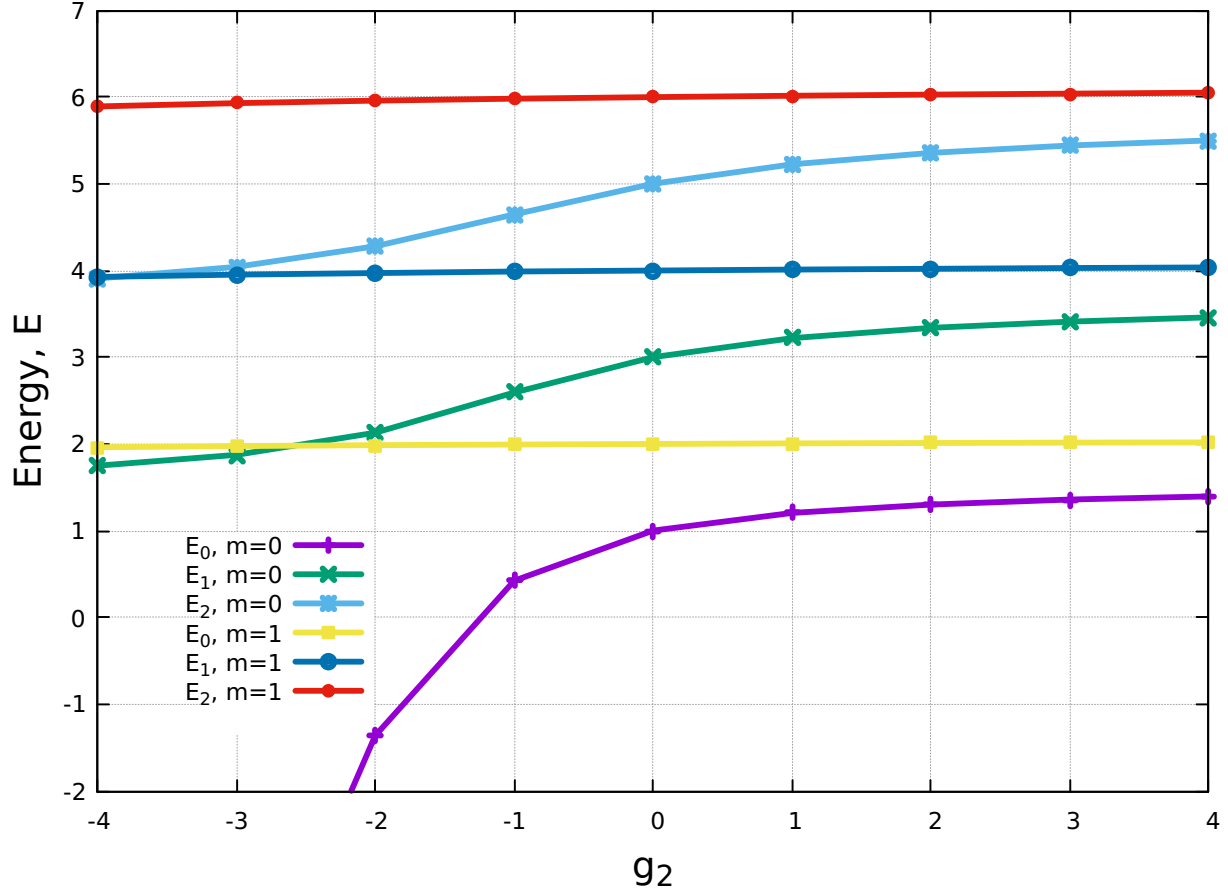


FIG. 7: (Colour online) Energy  $E$  in relative co-ordinates *vs* interaction strength  $g_2$ , for relative angular momentum  $|m| = 0$ , and 1, the interaction range  $\sigma = 0.1$  is plotted to study the energy-spectrum. Energy and  $g_2$  are units of  $\hbar\omega$  and  $\hbar^2/m$  respectively.

It is evident that the total energy  $E_0$  has large contribution from  $\langle KE \rangle + \langle PE \rangle$  as well. We have also observed that average interaction energy  $\langle V_0 \rangle$  increases with the increases in interaction strength for  $g_2 < 0$  and becomes saturated for  $g_2 > 0$ , on the other hand  $V_1$  and  $V_2$  first decreases then increases and then becomes constant for  $g_2 > 0$ . We also observed that at  $g_2 = 0$ , contribution is zero, means  $E_0 = \langle KE \rangle + \langle PE \rangle$  only has non-zero contribution. For  $g_2 < -1$  the  $\langle V_0 \rangle$  shows some un-physical trend. The ground energy  $V_0$  has very similar trend of the ground energy  $E_0$  in Fig. 7.

In Fig. 9, we plot the average interaction potential  $\langle V \rangle$  *vs* interaction strength  $g_2$  for relative angular momentum  $|m| = 1$  and interaction range  $\sigma = 0.1$ . The  $\langle V_0 \rangle$ ,  $\langle V_1 \rangle$  and  $\langle V_2 \rangle$  are the ground, first and the second excited state energy respectively. We have

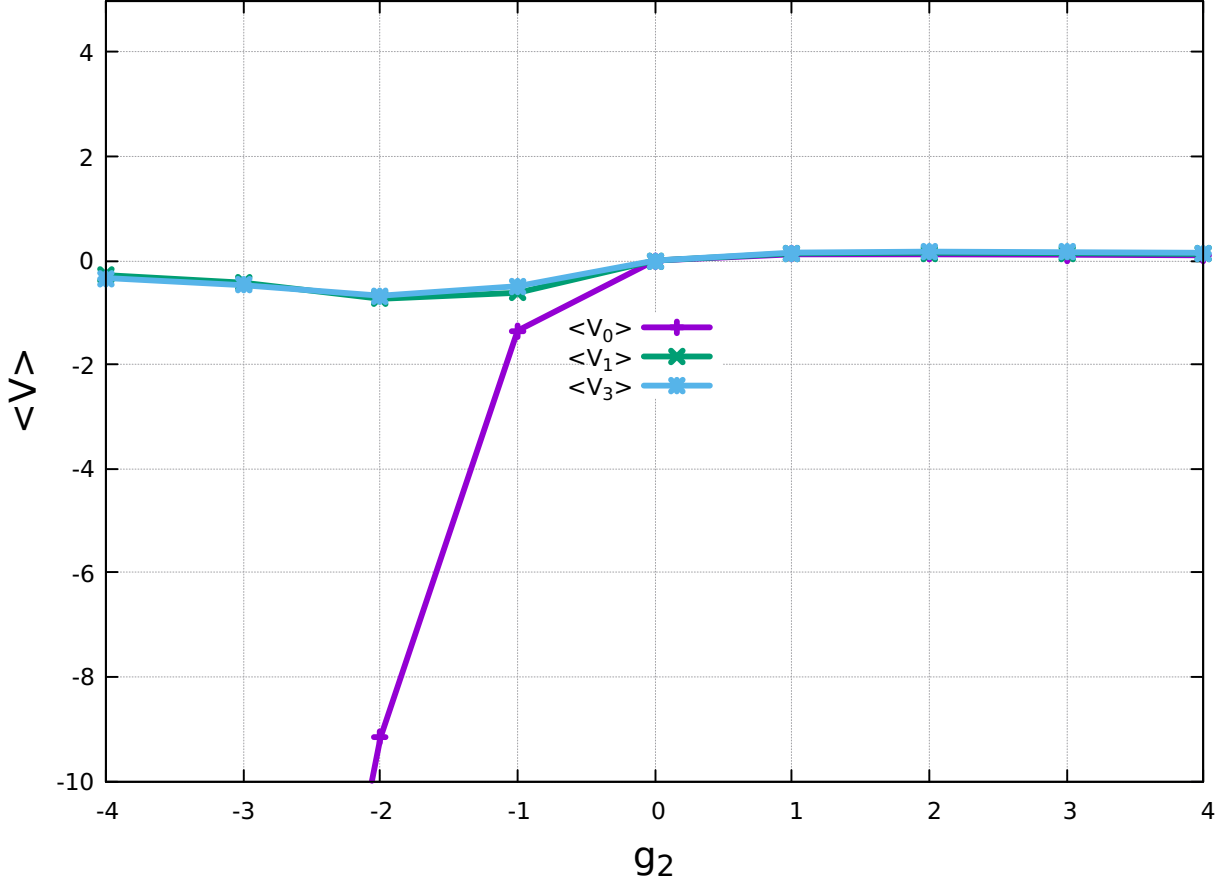


FIG. 8: (Colour online) The average interaction energy  $\langle V \rangle$  against interaction strength  $g_2$ , relative angular momentum ( $|m| = 0$ ) for the fixed interaction range  $\sigma$  is plotted to study the energy spectrum. The quantities  $\langle V_0 \rangle$ ,  $\langle V_1 \rangle$ ,  $\langle V_2 \rangle$  are being measured in units of  $\hbar\omega$  and  $\sigma$  is being measured in  $\sqrt{\frac{\hbar}{m\omega}}$  respectively.

observed that average interaction energy increases with the increases of interaction strength. We also observed that at  $g_2 = 0$ , contribution is zero, means  $E_0 = \langle KE \rangle + \langle PE \rangle$  only has non-zero contribution.

In Fig. 10, we plot ground state energy  $E_0$ , average interaction energy, kinetic energy and potential energy *vs* interaction strength  $g_2$  for relative angular momentum  $|m| = 0$ . In the interaction regime, we can not ignore in contribution of kinetic energy even for larger  $N$ , since it determines the structure of vortex core for larger  $N$ , in our case we observed that the contribution is dominant. In particular, the balance between the kinetic and the interaction energy fixes a typical distance over which the condensate wave function

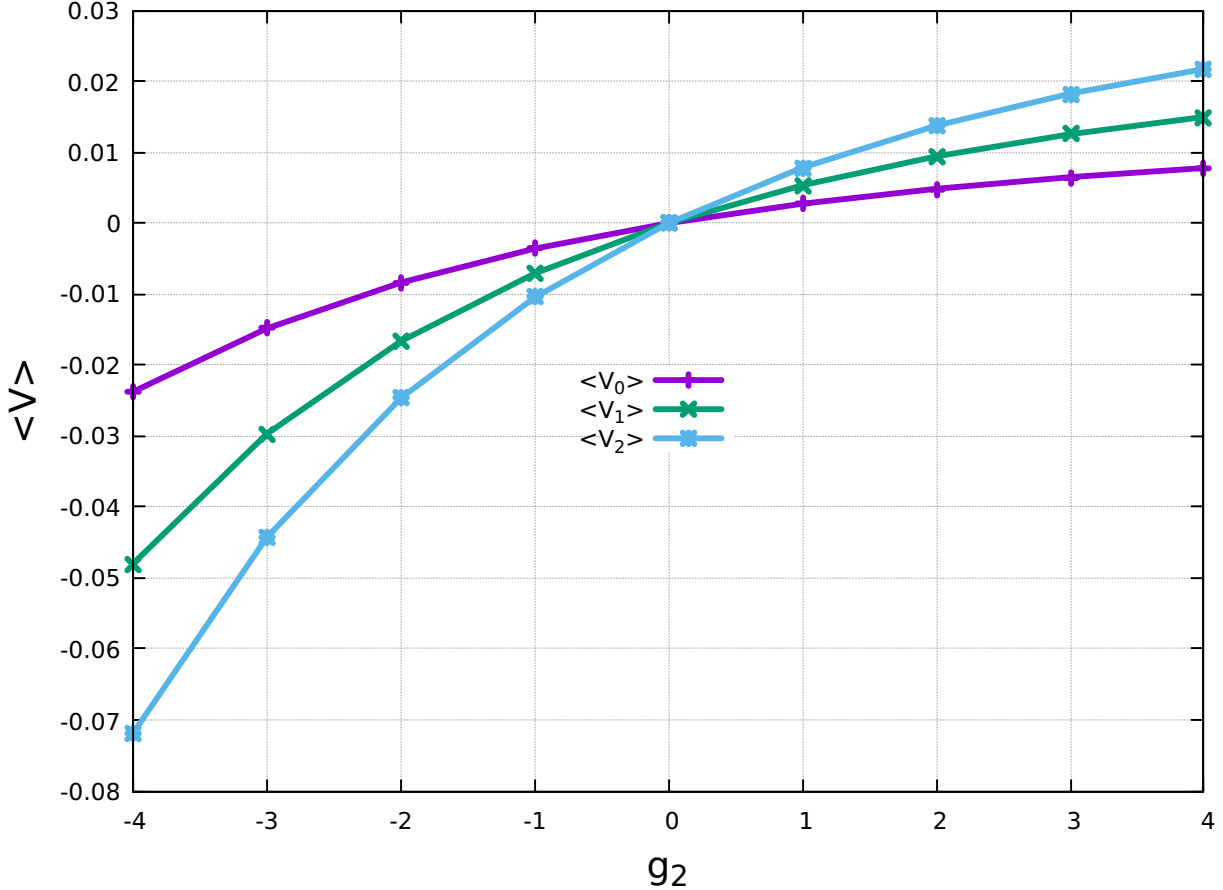


FIG. 9: (Colour online) The average interaction energy  $\langle V \rangle$  against interaction strength  $g_2$ , relative angular momentum ( $|m| = 1$ ) for the fixed interaction range  $\sigma$  is plotted to study the energy spectrum. The quantities  $\langle V_0 \rangle$ ,  $\langle V_1 \rangle$ ,  $\langle V_2 \rangle$  are being measured in units of  $\hbar\omega$  and  $\sigma$  is being measured in  $\sqrt{\frac{\hbar}{m\omega}}$  respectively.

can heal [? ]. Potential energy has the almost similar trend to the  $E_0$ . At  $g_2 = 0$ , the  $E_0 - \langle KE \rangle = E_0 - \langle PE \rangle = 1\hbar\omega$  and  $E_0 - \langle V \rangle = 2\hbar\omega$ . We also observed that the  $\langle V \rangle$  starts decreasing as the  $\langle KE \rangle$  started increasing for large value of  $g_2$ . Sum of all three energies, i.e.  $E_0 = \langle V \rangle + \langle KE \rangle + \langle PE \rangle$  contribution equals to the  $E_0$  irrespective of  $g_2$  and  $\sigma$ .

In Fig. 11, we plot ground state energy  $E_0$ , average interaction energy, kinetic energy and potential energy *vs* interaction strength  $g_2$  for non zero relative angular momentum  $m = 1$ . We have observed that the contribution of  $\langle KE \rangle = \langle PE \rangle$ , consider at  $g_2 = 0$ , but at the interactive interaction strength parameter  $g_2 = -4$  the  $\langle KE \rangle >$

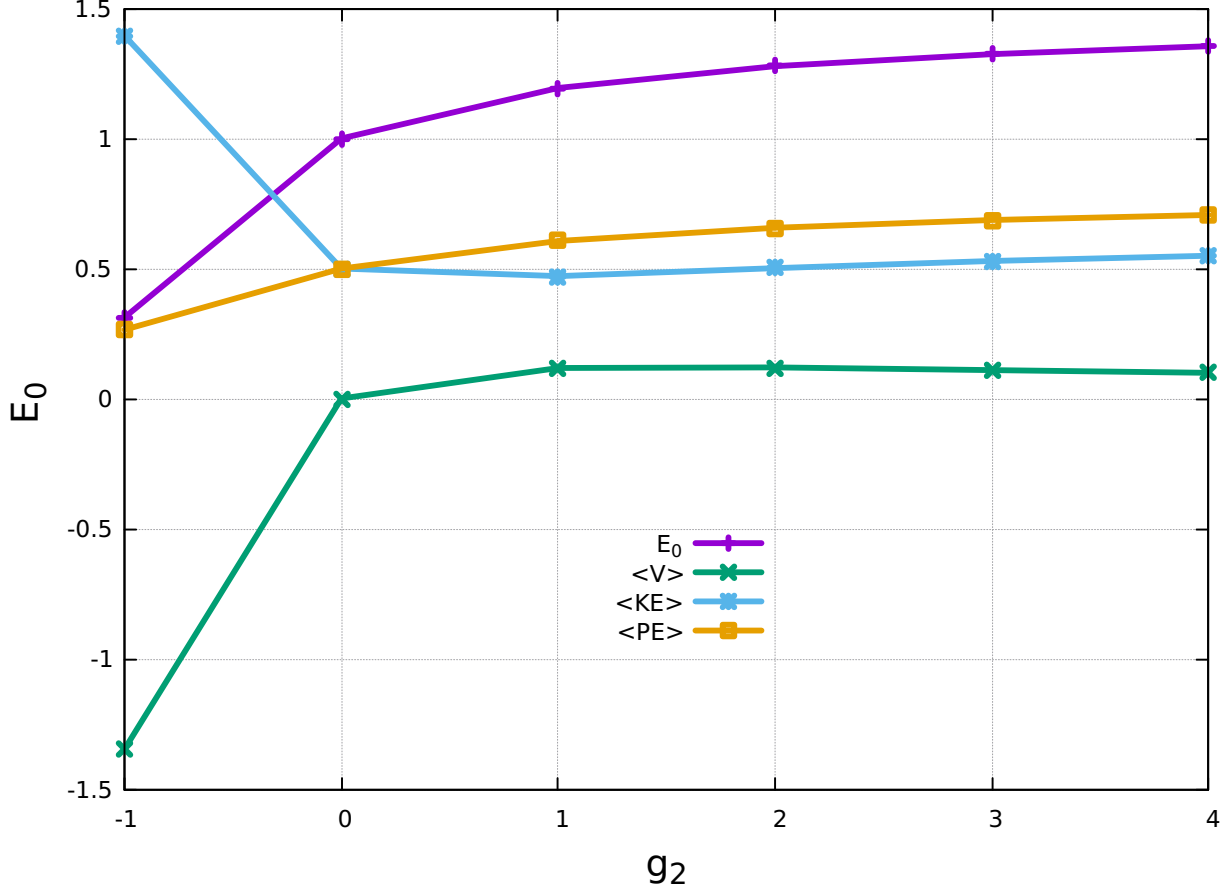


FIG. 10: (Colour online) Ground state energy  $E_0$  average interaction, kinetic and potential energy *vs* interaction parameter  $g_2$ , for relative angular momentum  $|m| = 0$ , is plotted to study the spectrum of energy, for active Hilbert space  $\tilde{N}_c = n_r = 80$ . The quantities  $E_0, \langle V \rangle, \langle KE \rangle, \langle PE \rangle$  are being measured in units of  $\hbar\omega$  and  $\sigma$  is being measured in  $\sqrt{\frac{\hbar}{m\omega}}$  respectively.

$\langle PE \rangle$  and opposite for repulsive  $g_2 = +4$ ,  $\langle KE \rangle < \langle PE \rangle$ . At  $g_2 = 0$ , the  $E_0 - \langle KE \rangle = E_0 - \langle PE \rangle = 1\hbar\omega$  and  $E_0 - \langle V \rangle = 2\hbar\omega$ . Sum of all three energies, i.e.  $\langle V \rangle + \langle KE \rangle + \langle PE \rangle$  contribution equals to the  $E_0$  for all  $g_2$ .

In Fig. 13, we plot ground state  $E_0$ , average interaction  $\langle V \rangle$ , kinetic energy  $\langle KE \rangle$  and potential energy  $\langle PE \rangle$  *vs* interaction range  $\sigma$  for interaction strength  $g_2 = -1$  and relative angular momentum  $m = 0$ . We have observed that the ground state energy  $E_0$  increases continuously and the same trend has been followed by the  $\langle V \rangle$ . The  $\langle KE \rangle$  is decreasing and gets saturated with system size. We observed that at  $\sigma = 0.4$ ,  $E_0 = \langle KE \rangle$

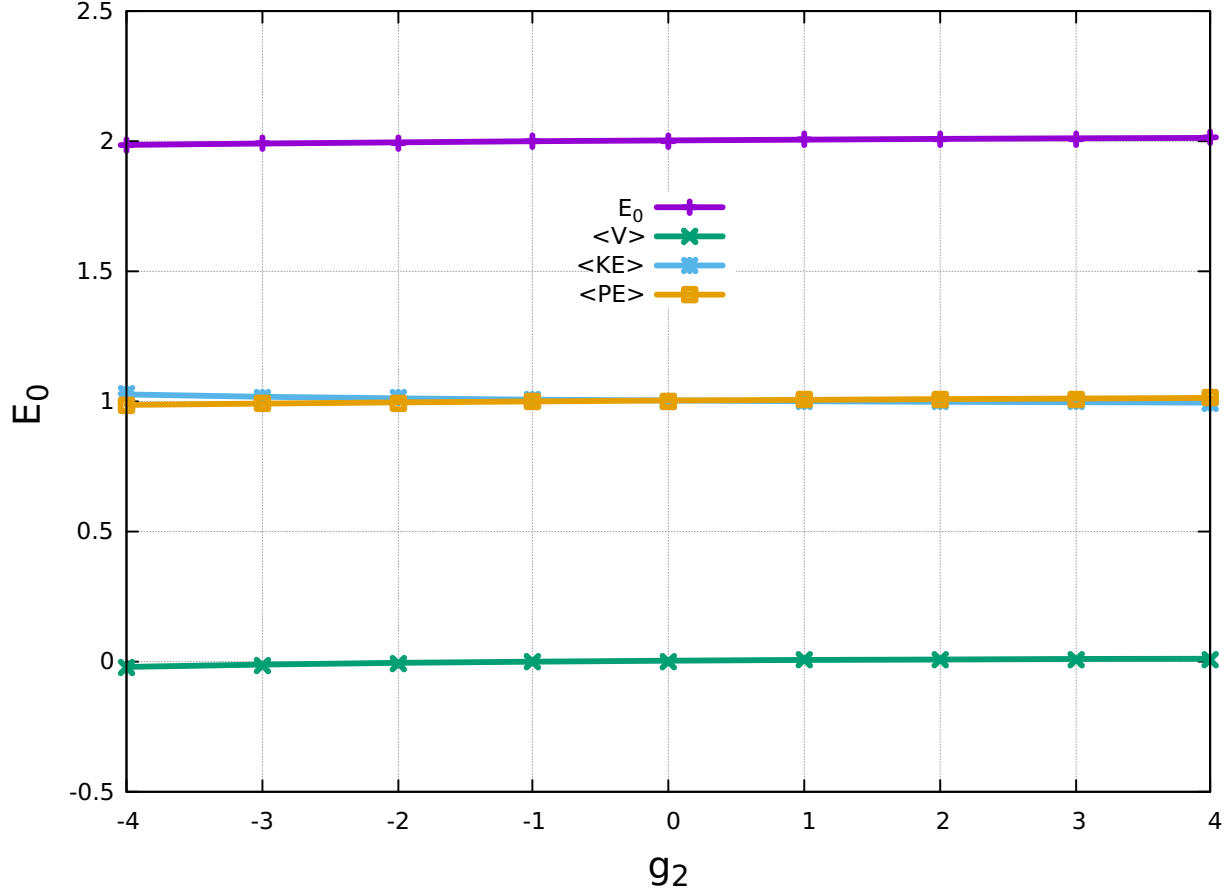


FIG. 11: (Colour online) Ground state energy  $E_0$  average interaction, kinetic and potential energy *vs* interaction parameter  $g_2$ , for relative angular momentum  $|m| = 1$ , is plotted to study the spectrum of energy, for active Hilbert space  $N_c = n_r = 80$ . The quantities  $E_0, \langle V \rangle, \langle KE \rangle, \langle PE \rangle$  are being measured in units of  $\hbar\omega$  and  $\sigma$  is being measured in  $\sqrt{\frac{\hbar}{m\omega}}$  respectively.

In Fig. 12, we plot ground state energy  $E_0$ , average interaction, kinetic energy and potential energy *vs* interaction range  $\sigma$ , for interaction strength  $g_2 = +1$  and relative angular momentum  $m = 0$ . For  $E_0$ , we have observed that the ground state energy, first increases and attains a peak at  $\sigma = 0.4$  and then starts decreasing for the system size.  $\langle V \rangle$  and  $\langle PE \rangle$  follow the same trend as of  $E_0$  on contrast the  $\langle KE \rangle$ , first decreases attains a minimum at  $\sigma = 0.4$  and then increases with system size. Sum of all three energies, i.e.  $\langle V \rangle + \langle KE \rangle + \langle PE \rangle$  contribution equals to the  $E_0$  for all  $\sigma$ .

and the rest net contribution from  $\langle PE \rangle$  and  $\langle V \rangle$  is 0. Sum of all three energies,

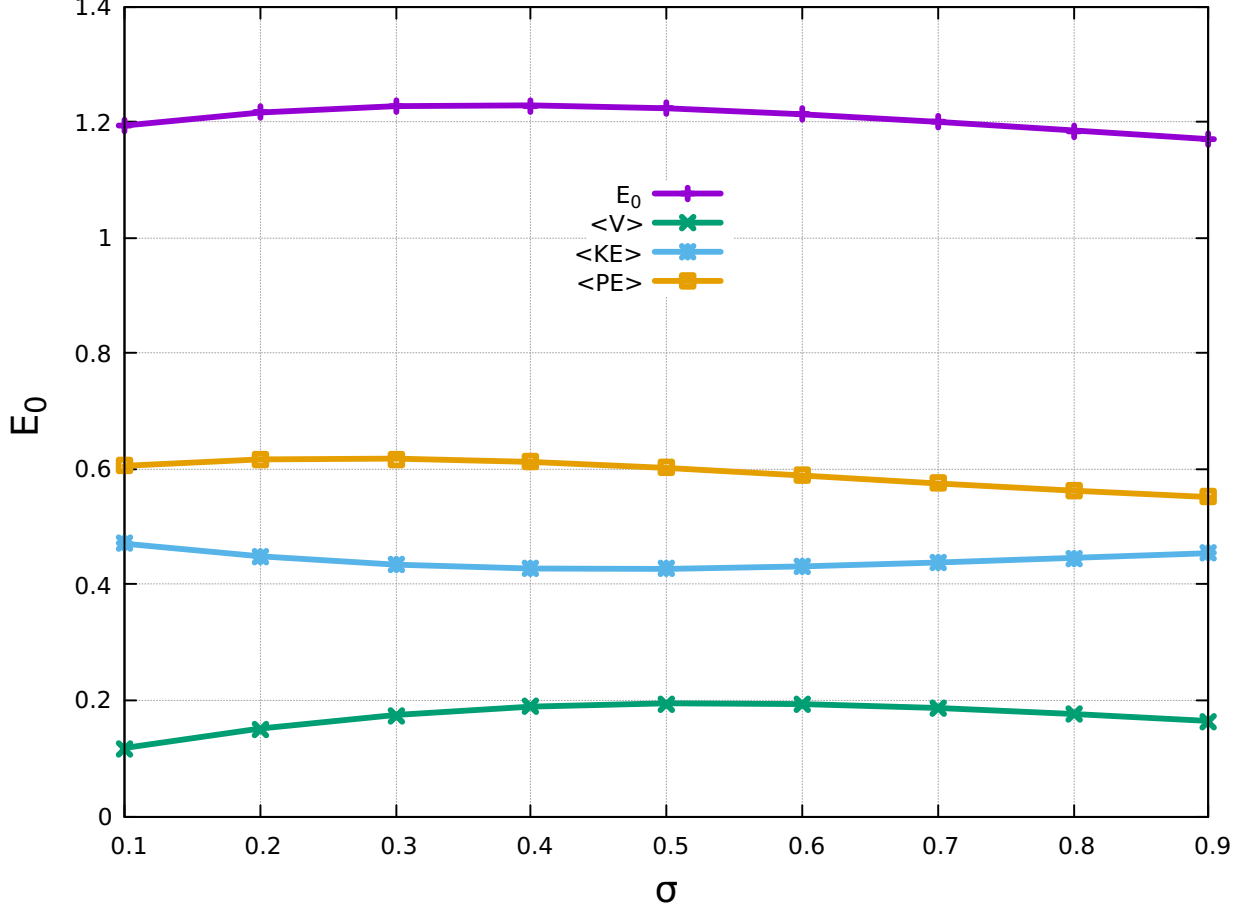


FIG. 12: (Colour online) Ground state energy  $E_0$ , average interaction, kinetic and potential, and trap potential energy *vs* interaction range  $\sigma$  for relative angular momentum  $|m| = 0$ , and interaction  $g_2 = +1$  is plotted to study the spectrum of energy, for active Hilbert space  $N_c = n_r = 80$ . The quantities  $E_0, \langle V \rangle, \langle KE \rangle, \langle PE \rangle$  are being measured in units of  $\hbar\omega$  and  $\sigma$  is being measured in  $\sqrt{\frac{\hbar}{m\omega}}$  respectively.

i.e.  $\langle V \rangle + \langle KE \rangle + \langle PE \rangle$  contribution equals to the  $E_0$  for all  $\sigma$ .

In Fig. 14, we plot ground state  $E_0$ , average interaction  $\langle V \rangle$ , kinetic energy  $\langle KE \rangle$  and potential energy  $\langle PE \rangle$  *vs* interaction range  $\sigma$  for interaction strength  $g_2 = -1$  and relative angular momentum  $m = 1$ . We have observed that the  $E_0, \langle V \rangle$  and  $\langle PE \rangle$  have been continuously increasing with system size in contrast with  $\langle KE \rangle$ , which is continuously decreasing. Sum of all three energies, i.e.  $\langle V \rangle + \langle KE \rangle + \langle PE \rangle$  contribution equals to the  $E_0$  for all  $\sigma$ .

In Fig. 15, we plot ground state  $E_0$ , average interaction energy  $\langle V \rangle$ , kinetic energy



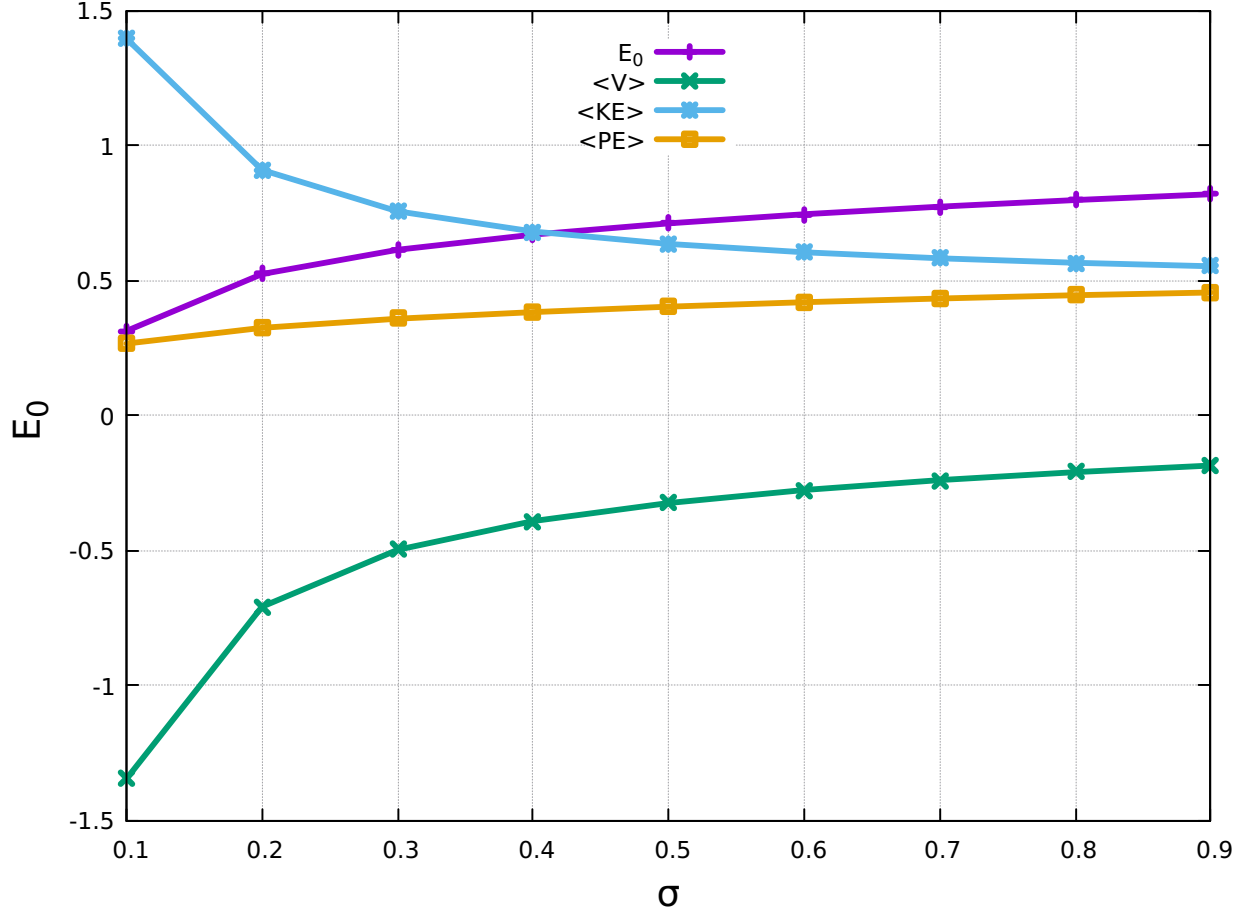


FIG. 13: (Colour online) Ground state energy  $E_0$ , average interaction, kinetic and potential, and trap potential energy *vs* interaction range  $\sigma$  for relative angular momentum  $|m| = 0$ , and interaction  $g_2 = -1$  is plotted to study the spectrum of energy, for active Hilbert space  $N_c = n_r = 80$ . The quantities  $E_0, \langle V \rangle, \langle KE \rangle, \langle PE \rangle$  are being measured in units of  $\hbar\omega$  and  $\sigma$  is being measured in  $\sqrt{\frac{\hbar}{m\omega}}$  respectively.

$\langle KE \rangle$  and potential energy  $\langle PE \rangle$  *vs* interaction range  $\sigma$  for interaction strength  $g_2 = -1$  and relative angular momentum  $m = 1$ . We have observed that the  $E_0, \langle V \rangle$  and  $\langle PE \rangle$  are continuously decreasing continuously decreasing in contrast to the  $\langle KE \rangle$ . Sum of all three energies, i.e.  $\langle V \rangle + \langle KE \rangle + \langle PE \rangle$  contribution equals to the  $E_0$  for all  $\sigma$ .

In the Fig. 16, we study the ground state energy  $E_0$  *vs* the interaction strength parameter  $g_2$ , for relative angular momentum  $|m|$  and the ratio of frequencies  $\Omega/\omega = 0.1$  for the different values of interaction range  $\sigma$ . For relative angular momentum  $|m| = 0$ , the

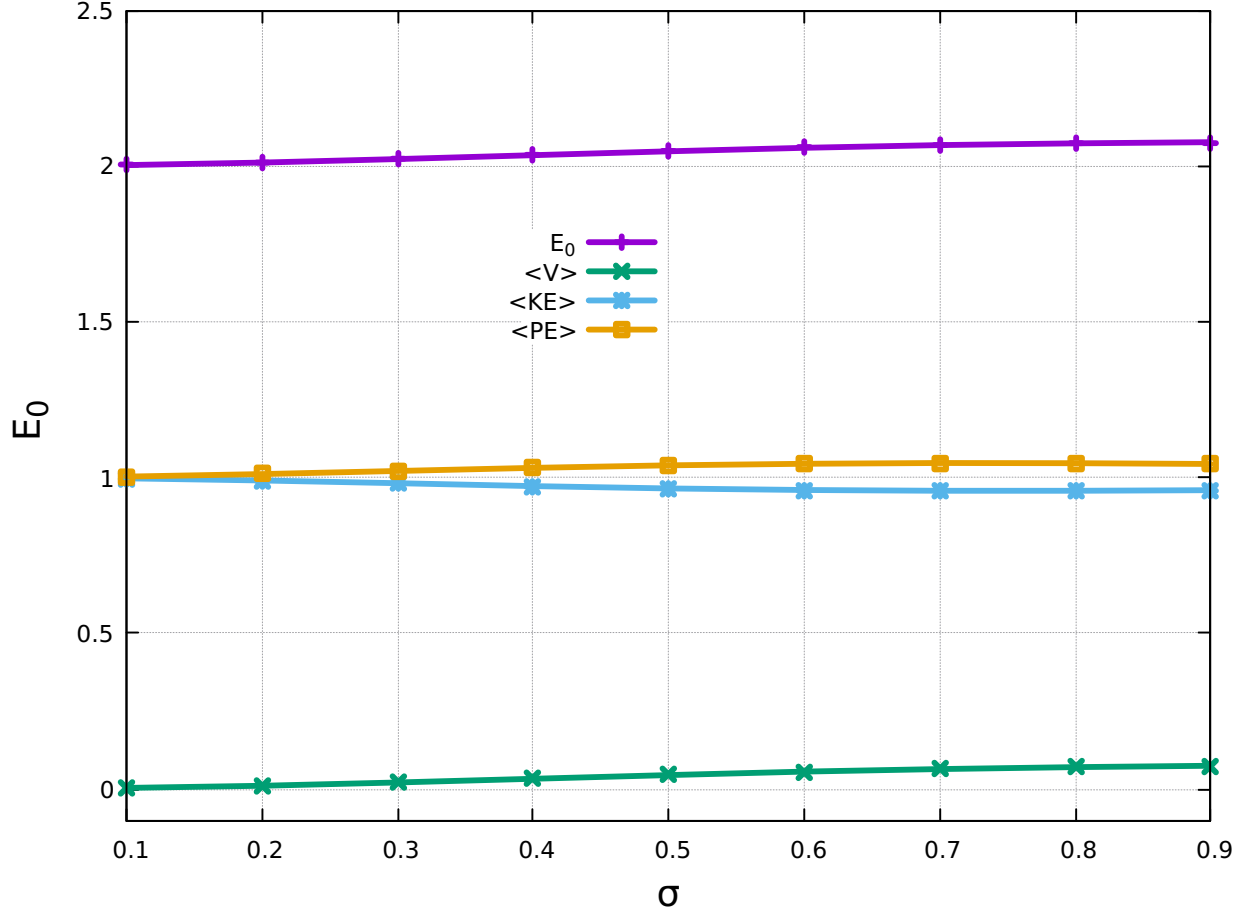


FIG. 14: (Colour online) Ground state energy  $E_0$ , average interaction, kinetic and potential, and trap potential energy *vs* interaction range  $\sigma$  for relative angular momentum  $|m| = 1$ , and interaction  $g_2 = +1$  is plotted to study the spectrum of energy, for active Hilbert space  $N_c = n_r = 80$ . The quantities  $E_0, \langle V \rangle, \langle KE \rangle, \langle PE \rangle$  are being measured in units of  $\hbar\omega$  and  $\sigma$  is being measured in  $\sqrt{\frac{\hbar}{m\omega}}$  respectively.

energy spectrum is slightly increasing with decreasing slope while for the relative angular momentum  $|m| = 1$  has the constant growth with constant slope. The energy increases with the increase in interaction range. There is an upward shift in energy with the increase in the relative angular momentum  $|m|$  from 0 to 1. There is an increase in energy gap with the increase in interaction strength.

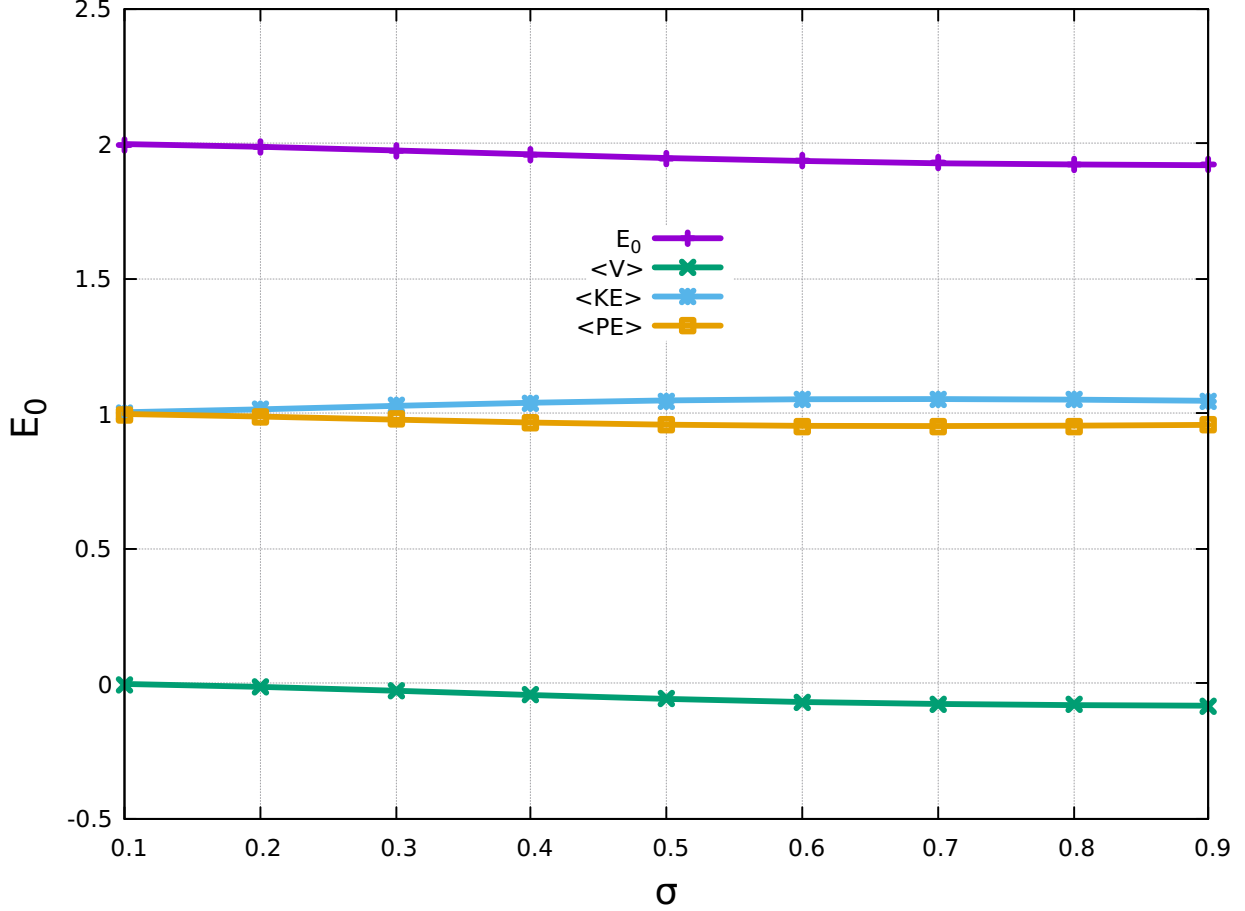


FIG. 15: (Colour online) Ground state energy  $E_0$ , average interaction, kinetic and potential, and trap potential energy *vs* interaction range  $\sigma$  for relative angular momentum  $|m| = 1$ , and interaction  $g_2 = -1$  is plotted to study the spectrum of energy, for active Hilbert space  $N_c = n_r = 80$ . The quantities  $E_0, \langle V \rangle, \langle KE \rangle, \langle PE \rangle$  are being measured in units of  $\hbar\omega$  and  $\sigma$  is being measured in  $\sqrt{\frac{\hbar}{m\omega}}$  respectively.

## VI. SUMMARY AND CONCLUSION

For the given systems of two-spin-0 bosons trapped in quasi 2-D harmonic trap in  $x - y$  symmetrical plane interacting via a finite range Gaussian potential. We analysed the ground state energy-spectrum in the subspace of single particle angular  $m$ . Allowing single particles angular momentum to takes both positive and negative values in single particle wave-function Eq. (A2). We have noted the energy spectrum for the both sign of  $|m| = 0$  and 1. We have explored the finite range interaction range  $\sigma$  and the interaction strength  $g_2$ . In the energy-spectrum study, the role of negative interaction strength has been extensively explored and

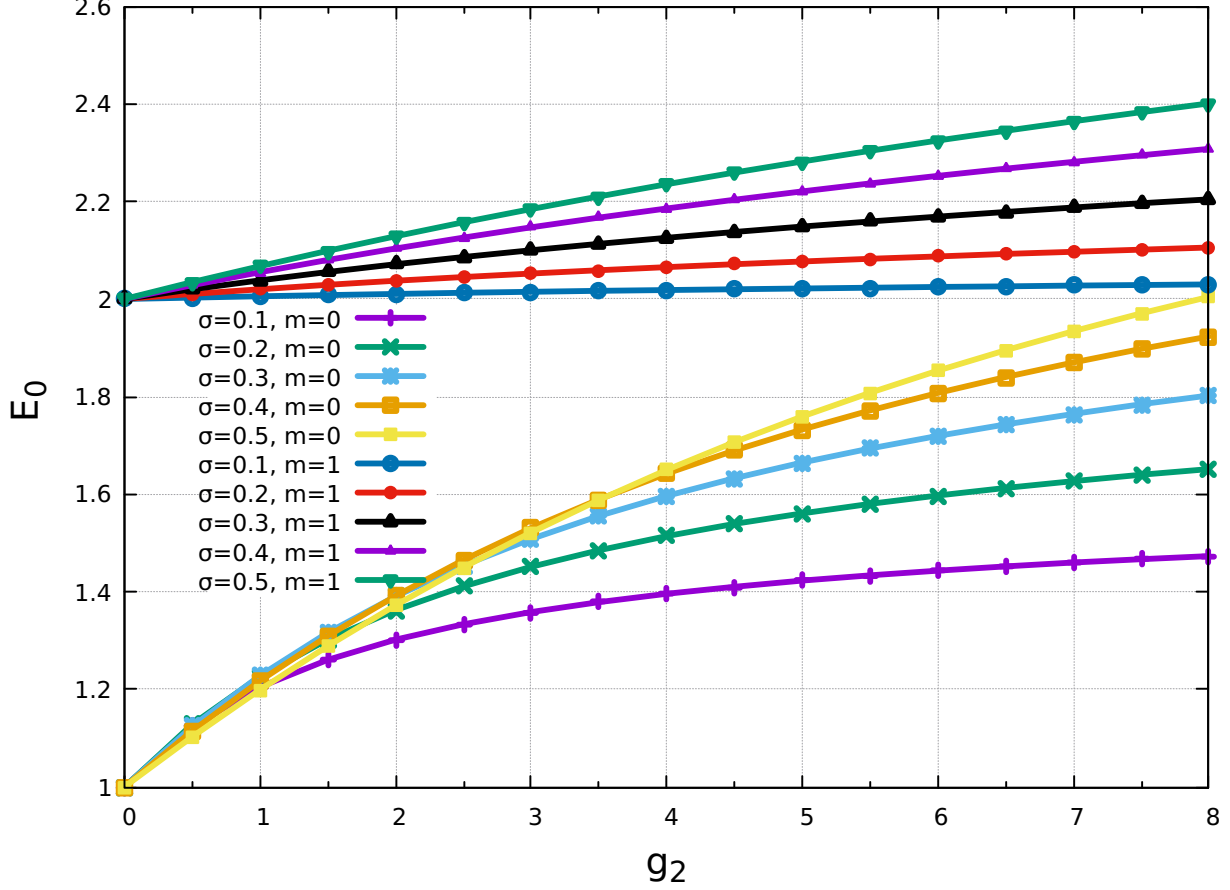


FIG. 16: (Color online) Ground state energy  $E_0$  in rotating  $|m| = 1$  and non-rotating  $|m| = 0$  as a function of interaction  $g_2$  and for the range  $\sigma = 0.1, 0.2, 0.3, 0.4$  and  $0.5$  is plotted to study the energy spectrum. The quantities  $E_0$  and  $g_2$  are being measured in units of  $\hbar\omega$ .

made a point that in the  $m = 0$  single particle angular momentum state, the energy spectrum  $\epsilon_{n_r} = 2n_r + |m| + 1 + \underbrace{g_2 V(r)}_g - m\Omega/\omega_\perp$ , that for non-rotating case, we terminate our study at  $g < -1$  because, since, energy in the units of  $1\hbar\omega$  is the zero-point energy of a system of two spin-0 bosons in relative co-ordinates. For  $g \leq -1\hbar\omega$ , the system forms a bound state with energy  $< 0$ . At strength  $g_2 < -1$  turns the system into a lump which becomes independent of the quantum statistics and hence no further interaction will make any physical meaning, therefore we terminate our study at strength  $g = -1$ . In rotating case  $m = 1$  has freedom in the sense that the strength  $g = -(1 + |m| - m\Omega/\omega_\perp)$  can have different values because there is no violation of quantum statistics. We have studied the total ground state energy in

terms of various components like trap potential, and interaction potential energy  $PE, KE$  and  $\langle V \rangle$ . We have observed that the variation in the  $\langle PE \rangle$ , with respect to  $\langle KE \rangle$  and  $\langle V \rangle$  is very small.

### Appendix A: Calculation of interaction matrix elements

In this appendix we outline the steps for calculation of the matrix elements used in the secular equation in the main text, at equation 1.8, for that we consider a normalised single particle wavefunction  $u_{n_r, m}(r_\perp \alpha_\perp, \phi)$  in relative co-ordinates and integrate it over  $r dr d\phi$ , where,  $r$  is spatial relative co-ordinate and  $\phi$  is azimuthal angle. The single particle interaction elements is being calculated in the following manner. The matrix elements is written in the following way.

$$I_{n_r, n_r', |m|}(\sigma) = \langle u_{n_r, m}(r_\perp \alpha_\perp, \phi) | V(r) | u_{n_r', m'}(r_\perp \alpha_\perp, \phi) \rangle \quad (\text{A1})$$

and the single particle wavefunction,

$$\begin{aligned} u_{n_r, m}(r_\perp \alpha_\perp, \phi) &= \sqrt{\frac{\alpha_\perp^2 n_r!}{\pi(n_r + |m|)!}} (r_\perp \alpha_\perp)^{|m|} e^{-\frac{1}{2} r_\perp^2 \alpha_\perp^2} \\ &\times e^{im\phi} L_{n_r}^{|m|}(r_\perp^2 \alpha_\perp^2) \end{aligned} \quad (\text{A2})$$

where,  $L_{n_r}^{|m|}(r_\perp^2 \alpha_\perp^2)$  is the associated Laguerre polynomials,

$$\begin{aligned} &= \int_0^\infty \int_0^{2\pi} r_\perp dr_\perp d\phi \sqrt{\frac{\alpha_\perp^2 n_r!}{\pi(n_r + |m|)!}} \\ &\times (r_\perp \alpha_\perp)^{|m|} e^{-1/2 r_\perp^2 \alpha_\perp^2} e^{im\phi} \\ &\times L_{n_r}^{|m|}(r_\perp^2 \alpha_\perp^2) \times \frac{1}{2\pi\sigma^2} \exp\left(-\frac{r^2}{2\sigma^2}\right) \\ &\times \sqrt{\frac{\alpha_\perp^2 n_r'!}{\pi(n_r' + |m'|)!}} (r_\perp \alpha_\perp)^{|m'|} \\ &\times e^{-1/2 r_\perp^2 \alpha_\perp^2} e^{-im'\phi} L_{n_r'}^{|m'|}(r_\perp^2 \alpha_\perp^2) \end{aligned}$$

the integration is being carried out for the  $\phi$  first, which gives delta function,

$$\begin{aligned}
&= \frac{1}{2\pi\sigma^2} \int r_{\perp} dr_{\perp} 2\pi\delta(m - m') \sqrt{\frac{\alpha_{\perp}^2 n_r!}{\pi(n_r + |m|)!}} \\
&\times (r_{\perp}\alpha_{\perp})^{|m|} e^{-1/2r_{\perp}^2\alpha_{\perp}^2} L_{n_r}^{|m|}(r_{\perp}^2\alpha_{\perp}^2) \\
&\times \sqrt{\frac{\alpha_{\perp}^2 n_r'!}{\pi(n_r' + |m'|)!}} (r_{\perp}\alpha_{\perp})^{|m'|} e^{-1/2r_{\perp}^2\alpha_{\perp}^2} L_{n_r'}^{|m'|}(r_{\perp}^2\alpha_{\perp}^2)
\end{aligned}$$

using property of the Dirac-delta function we can substitute  $m = m'$  and rearranging the normalization constants the integration over relative co-ordinate is to be carried out in the following manner,

$$\begin{aligned}
&= \sqrt{\frac{n_r!}{\pi(n_r + |m|)!}} \sqrt{\frac{n_r'!}{\pi(n_r' + |m|)!}} \pi \frac{1}{2\pi\sigma^2} \int \underbrace{\alpha_{\perp}^2 2r_{\perp} dr_{\perp}}_{d(r_{\perp}^2\alpha_{\perp}^2)} \\
&\times (r_{\perp}\alpha_{\perp})^{2|m|} \exp(-r_{\perp}^2\alpha_{\perp}^2(1 + \frac{1}{2\alpha^2\sigma^2})) L_{n_r'}^{|m|}(r_{\perp}^2\alpha_{\perp}^2) \\
&\times L_{n_r}^{|m|}(r_{\perp}^2\alpha_{\perp}^2)
\end{aligned}$$

assuming the dimensionless quantity

$$1 + \frac{1}{2\alpha^2\sigma^2} = \Lambda$$

and rewriting the integrand in the terms of  $\Lambda$ ,

$$\begin{aligned}
&= \sqrt{\frac{n_r!}{\pi(n_r + |m|)!}} \sqrt{\frac{n_r'!}{\pi(n_r' + |m|)!}} \pi \frac{1}{2\pi\sigma^2} \int d(\alpha_{\perp}^2 r_{\perp}^2) \\
&\times (r_{\perp}\alpha_{\perp})^{2|m|} \exp(-r_{\perp}^2\alpha_{\perp}^2\Lambda) L_{n_r'}^{|m|}(r_{\perp}^2\alpha_{\perp}^2) L_{n_r}^{|m|}(r_{\perp}^2\alpha_{\perp}^2)
\end{aligned}$$

again defining  $r_{\perp}^2\alpha_{\perp}^2\Lambda = \rho$  in form of new dimensionless parameter and substituting it in the above expression which further simplify to,

$$\begin{aligned}
&= \frac{1}{2\pi\sigma^2\Lambda} \sqrt{\frac{n_r!}{(n_r + |m|)!} \frac{n_r'!}{(n_r' + |m|)!}} \int d\rho \\
&\times \left(\frac{\rho}{\Lambda}\right)^{|m|} \exp(-\rho) L_{n_r'}^{|m|}\left(\frac{\rho}{\Lambda}\right) L_{n_r}^{|m|}\left(\frac{\rho}{\Lambda}\right)
\end{aligned}$$

and rescaling parameters gives,

$$\begin{aligned}
&= \frac{1}{2\pi\sigma^2 \Lambda^{1+|m|}} \sqrt{\frac{n_r!}{(n_r + |m|)!} \frac{n_r'!}{(n_r' + |m|)!}} \int d\rho \\
&\times \rho^{|m|} \exp(-\rho) L_{n_r'}^{|m|}\left(\frac{\rho}{\Lambda}\right) L_{n_r}^{|m|}\left(\frac{\rho}{\Lambda}\right)
\end{aligned}$$

using multiplication formula for the associated Laguerre polynomials in the above integral to make it solvable by removing  $1/\Lambda$  term from it [29]

$$L_{n_r}^{[m]}(\Lambda x) = \sum_{i=0}^{n_r} \frac{\Lambda^i (|m|+1)_{n_r} (1-\Lambda)^{n_r-i}}{(|m|+1)_i (n_r-i)!} L_i^{[m]}(x)$$

writing the expression in Pochhammer symbols, the integrand is now function of single variable  $\rho$  which can be easily solved,

$$\begin{aligned} &= \frac{1}{2\pi\sigma^2\Lambda^{1+|m|}} \sqrt{\frac{n_r!}{(n_r+|m|)!} \frac{n_r'!}{(n_r'+|m|)!}} \\ &\times \sum_{i,i'=0}^{\min(n_r,n_r')} \frac{\Lambda^{-i-i'} (|m|+1)_{n_r} (1-\Lambda^{-1})^{n_r+n_r'-i-i'}}{(|m|+1)_i (n_r-i)!} \\ &\times \frac{(|m|+1)_{n_r'}}{(|m|+1)_{i'} (n_r'-i')!} \int_0^\infty d\rho \rho^{|m|} \exp(-\rho) L_i^{[m]}(\rho) L_{i'}^{[m]}(\rho) \end{aligned}$$

using the orthogonality condition for the associated Laguerre polynomials, the expression becomes,

$$\begin{aligned} &= \frac{1}{2\pi\sigma^2\Lambda^{1+|m|}} \sqrt{\frac{n_r!}{(n_r+|m|)!} \frac{n_r'!}{(n_r'+|m|)!}} \\ &\times \left(\frac{\Lambda-1}{\Lambda}\right)^{n_r+n_r'} \sum_{i=0}^{\min(n_r,n_r')} \frac{(|m|+1)_{n_r}}{(|m|+1)_i (n_r-i)!} \\ &\times \frac{(|m|+1)_{n_r'}}{(|m|+1)_i (n_r'-i)!} \frac{(i+|m|)!}{i!} \left(\frac{1}{(\Lambda-1)^2}\right)^i \end{aligned}$$

writing the Pochhammer symbol in the terms of factorials,  $(a)_n = \frac{(a+n-1)!}{(a-1)!}$  we have the following results.

$$\begin{aligned} I_{n_r,n_r',|m|}(\sigma) &= \frac{1}{2\pi\sigma^2\Lambda^{1+|m|}} \sqrt{\frac{n_r!}{(n_r+|m|)!} \frac{n_r'!}{(n_r'+|m|)!}} \\ &\times \left(\frac{\Lambda-1}{\Lambda}\right)^{n_r+n_r'} \sum_{i=0}^{\min(n_r,n_r')} \binom{|m|+n_r}{|m|+i} \\ &\times \binom{|m|+n_r'}{|m|+i} \frac{(|m|+i)!}{i!} \left(\frac{1}{(\Lambda-1)^2}\right)^i. \end{aligned}$$

(A3)

this results will be useful in the further study of problems in the main text with the original parameters.

## Appendix B: Calculation of constant $c_{n_r,m}$ .

In this section we perform the calculation for the expansion co-efficient used at Eq. 1.8 in main text, however the approach is general and can be found in any standard quantum mechanics text. We solve the following Hamiltonian operator in simple way, A different approach is given in [33].

$$\hat{H} = \underbrace{\hat{H}_0 - \Omega \cdot \hat{\mathbf{L}}}_{H_{sp}} + g_2 W$$

where the  $H_{sp}$  is single particle Hamiltonian, we write the wavefunction in the product form of expansion co-efficient and single particle wave-function,

$$|\psi_{n_r,m}\rangle = \sum_{n_r,m} c_{n_r,m} u_{n_r,m} \quad (\text{B1})$$

as the eigenenergy and eigenstates of unperturbed Hamiltonian is known to be.  $H_{sp}|u_{n_r,m}\rangle = \epsilon_{n_r,m}|u_{n_r,m}\rangle$ ,

$$\begin{aligned} (H_{sp} + g_2 W)|\psi\rangle &= E|\psi\rangle \\ (E - H_{sp})|\psi\rangle &= g_2 W|\psi\rangle \end{aligned}$$

on operating  $|u_{n_r,m}\rangle$  from right we get the following form

$$(E - \epsilon_{n_r,m})\langle u_{n_r,m}|\psi\rangle = g_2 \langle u_{n_r,m}|W|\psi\rangle \quad (\text{B2})$$

from the above equation we get the expansion coefficients,

$$c_{n_r,m} = \langle u_{n_r,m}|\psi\rangle = \frac{g_2 \langle u_{n_r,m}|W|\psi\rangle}{E - \epsilon_{n_r,m}} \quad (\text{B3})$$

till now no approximation has been used, unknown  $|\psi\rangle$  in above equation is dependent on the co-efficient. We can set  $|\psi\rangle = |u_{0,m}\rangle$  and  $|\psi\rangle = |u_{r',m}\rangle$  for the study of ground and excited states respectively in A.4. The ground state

$$c_{n_r,m} = -\frac{g_2 \langle u_{n_r,m}|W|u_{0,m}\rangle}{(\epsilon_{n_r,m} - E)} \quad (\text{B4})$$

and the most general form for studying the higher excited states,

$$c_{n_r,m} = -\frac{g_2 \langle u_{n_r,m}|W|u_{n_r',m}\rangle}{(\epsilon_{n_r,m} - E)}. \quad (\text{B5})$$

we can arrive to the exact and approximate solution in the main text.



### Appendix C: Expectation of trap potential.

This expectation gives the matrix elements for the trapping potential of harmonic oscillator, this calculation is based on the basic quantum mechanics technique and can be found in any standard text book.

$$\begin{aligned}
\langle \alpha^2 r^2 \rangle &= \int_0^\infty \int_0^{2\pi} r_\perp dr_\perp d\phi \sqrt{\frac{\alpha_\perp^2 n_r!}{\pi(n_r + |m|)!}} \\
&\times (r_\perp \alpha_\perp)^{|m|} e^{-1/2r_\perp^2 \alpha_\perp^2} e^{im\phi} \\
&\times L_{n_r}^{|m|}(r_\perp^2 \alpha_\perp^2) \times r^2 \alpha^2 \\
&\times \sqrt{\frac{\alpha_\perp^2 n_r'!}{\pi(n_r' + |m'|)!}} \\
&\times (r_\perp \alpha_\perp)^{|m'|} e^{-1/2r_\perp^2 \alpha_\perp^2} e^{-im'\phi} \\
&\times L_{n_r'}^{|m'|}(r_\perp^2 \alpha_\perp^2)
\end{aligned}$$

first we have integrated over the  $\phi$  and from there a factor of  $2\pi\delta_{m,m'}$  simplify the integration in the following way, similar steps as in the earlier calculations

$$\begin{aligned}
&= \sqrt{\frac{n_r'! n_r!}{(n_r + |m|)!(n_r' + |m|)!}} \int_0^\infty d(\alpha_\perp^2 r_\perp^2) (r_\perp^2 \alpha_\perp^2)^{|m|+1} \\
&\times e^{-r_\perp^2 \alpha_\perp^2} L_{n_r}^{|m|}(r_\perp^2 \alpha_\perp^2) L_{n_r'}^{|m|}(r_\perp^2 \alpha_\perp^2)
\end{aligned}$$

using orthogonality relation of associated Laguerre polynomials,

$$= \sqrt{\frac{n_r'!(n_r + |m|)!}{n_r!(n_r' + |m|)!}} (2n_r + |m| + 1) \tag{C1}$$

for  $m = 0$  the above equation simplyfy to the simple form  $2n_r + 1$ .

- 
- [1] S. N Bose, Z. Phys. **26**, 0178 (1924).
  - [2] Einstein, Klasse. (1924) p. 261; (1925) p. 3, 0178 (1924).
  - [3] F London, Nature. **141**, 0643 (1938).
  - [4] Eloisa Cuesta, Martin D Jimenez and Ana P Majtey, J. Phys. A: Math. Theor. **54**, 025302 (2021).
  - [5] Y. S. Li, B. Zeng, X. S. Liu and G.L. Long Phys. Rev. A **64**, 054302 (2001) .

- [6] K. D. Sen, H. E. Montgomery Jr, Bowen Yu and Jacob Katriel, Eur. Phys J. D, **75**, 175, (2021).
- [7] Thomas Busch, Berthold-Georg Englert, Kszimierz Rzazewski and Martin Wilkens, Found. of Phys, **28**, 550, (1998).
- [8] Rostislav A. Doganov, Shachar Klaiman, Ofir E. Alon, Alexej I. Streltsov and Lorenz S. Cederbaum, Phys. Rev A **87**,033631-1 (2013).
- [9] Mohd Imran and M A H Ahsan, J. Phys. B: At. Mol. Opt. Phys **53**,125303 (2020).
- [10] J. Christensson, C. Forssen, S. Aberg and S. M. Reimann, Phys. Rev A, **79**, 012707 (2009)
- [11] Shu-Wei Song, Yi-Cai Zhang, Hong Zho, Xuan Wang and Wu-Ming Liu, Phys. Rev A, **89**, 063613 (2014)
- [12] Hiroki Saito and Masahito Ueda, Phys. Rev Lett, **89**, 190402 (2002)
- [13] Abel Rojo-Francäs, Artur Polls and Bruno Juliä-Díaz, Mathematics **8**,(2020) 1196.
- [14] S. Inouye, M.R. Andrews,J.Stanger, H.J.Miesner, D.M. Stamper-Kurn and W. Ketterle, Nature (London) **392**,(1998) 151.
- [15] A.D.Lange, K.Pilch, A. Pranter, F.Ferlaino, B. Engeser, H.-C. Nägerl, R. Grsimmm and C. Chin,Phys. Rev A, **79**, 013622 (2009).
- [16] Luca Salasnich and Boris A. Malomed, Phys. Rev. A **79**, (2009), 053620.
- [17] F. Dalfovo, S. Giorgini, L. P. Pitaevskii and S. Strongari, Rev Mod. Phys. **71**, (1999), 463.
- [18] Przemyslaw Koscik and Tomasz. Sowinsk. Scientific reports **8**,18505 (2018)
- [19] Thomas Thomas, Berthold-Georg Englert, Kazimierz Rzazewski and Kazimierz Wilkens. Foundations of Physics,**549**, 498 (1997).
- [20] Pere Mujal, Artur Polls and B Juliä-Díaz, Phys. Rev. Lett., **97**, 063618, (2018)
- [21] Shachar Klaiman, Nimrod Moiseyev and Lorenz S Cederbaum. Phys. Rev. A **73**, 013622 (2006).
- [22] Ernest R Davison, Rev. Mod. Phys, **44**, 451, (1972).
- [23] M. A. H. Ahsan and N. Kumar, Phys. Rev. A **64**, 013608 (2001).
- [24] Anna Dawid, Maciej Lewenstein, and Michał Tomza, Phys. Rev A, **97**, 063618 (2018).
- [25] E. Garrido and A. S. Jensen, Phys. Rev. Research **2**, 033261 (2020).
- [26] Peter Jeszenszki. Ali. Alavi and Joachin Brand, Phys. Rev. A **99**, 033608 (2019).
- [27] Xia-Ji Liu, Hui Hu, Lee Chang and Shi-Qun Li, Phys. Rev A, **64**, 035601 (2001)
- [28] Pere Mujal, Enric Sarle, Artur Polls, and B Juliä-Díaz, Phys. Rev. A **96**, 043614 (2017).

- [29] D.D Tcheutia, M. Foupouagnigni, W. Koepf, P. Njionou Sadjang, *The Ramanujan J.* , (2016), 498.
- [30] Xia-Ji Liu, Hui Hu and Peter D. Drummond, *Phys. Rev B*, **82**, 054524 (2010).
- [31] A. Roussou et. al *Phys Rev A* **99**, 053613 (2019)
- [32] Ernest R Davison, *Rev. Mod. Phys*, **44**, 451, (1972).
- [33] Xia-Ji Liu, Hui Hu and Peter D. Drummond, *Phys. Rev B*, **82**, 054524 (2010).